JOINT TRANSPORTATION
RESEARCH PROGRAM
INDIANA DEPARTMENT OF TRANSPORTATION
AND PURDUE UNIVERSITY

Environmentally Tuning Asphalt Pavements Using Phase Change Materials

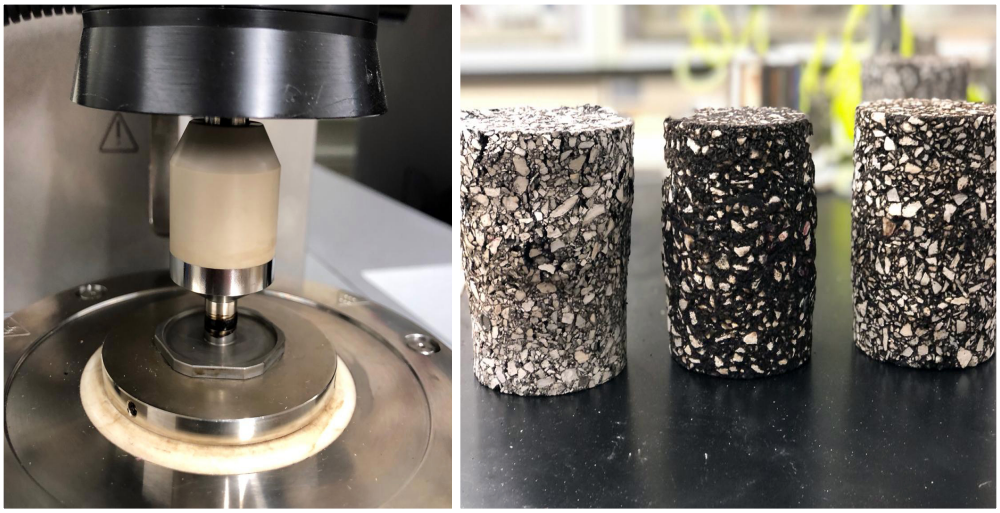

Miguel A. Montoya, Daniela Betancourt-Jimenez, Mohammad Notani,
Reyhaneh Rahbar-Rastegar, Jeffrey P. Youngblood,
Carlos J. Martinez, John E. Haddock

SPR-4335 • Report Number: FHWA/IN/JTRP-2022/06 • DOI: 10.5703/1288284317369

RECOMMENDED CITATION

Montoya, M. A., Betancourt-Jimenez, D., Notani, M., Rahbar-Rastegar, R., Youngblood, J. P., Martinez, C. J., & Haddock, J. E. (2022). *Environmentally tuning asphalt pavements using phase change materials* (Joint Transportation Research Program Publication No. FHWA/IN/JTRP-2022/06). West Lafayette, IN: Purdue University. https://doi.org/10.5703/1288284317369

AUTHORS

Miguel A. Montoya
Daniela Betancourt-Jimenez
Mohammad Notani
Graduate Research Assistants
Lyles School of Civil Engineering
Purdue University

Reyhaneh Rahbar-Rastegar, PhD
Research Engineer
Lyles School of Civil Engineering
Purdue University

Jeffrey P. Youngblood, PhD
Professor of Materials Engineering
School of Materials Engineering
Purdue University

Carlos J. Martinez, PhD
Associate Professor of Materials Engineering
School of Materials Engineering
Purdue University

John E. Haddock, PhD, PE
Professor of Civil Engineering
Director of Indiana Local Technical Assistance Program
Lyles School of Civil Engineering
Purdue University
(765) 496-3996
jhaddock@purdue.edu
Corresponding Author

JOINT TRANSPORTATION RESEARCH PROGRAM

The Joint Transportation Research Program serves as a vehicle for INDOT collaboration with higher education institutions and industry in Indiana to facilitate innovation that results in continuous improvement in the planning, design, construction, operation, management and economic efficiency of the Indiana transportation infrastructure. https://engineering.purdue.edu/JTRP/index_html

Published reports of the Joint Transportation Research Program are available at http://docs.lib.purdue.edu/jtrp/.

NOTICE

TECHNICAL REPORT DOCUMENTATION PAGE

1. Report No. FHWA/IN/JTRP-2022/06	**2. Government Accession No.**	**3. Recipient's Catalog No.**
4. Title and Subtitle Environmentally Tuning Asphalt Pavements Using Phase Change Materials		**5. Report Date** February 2022 **6. Performing Organization Code**
7. Author(s) Miguel Montoya, Daniela Betancourt-Jimenez, Mohammad Notani, Reyhaneh Rahbar-Rastegar, Jeffrey P. Youngblood, Carlos J. Martinez, and John E. Haddock		**8. Performing Organization Report No.** FHWA/IN/JTRP-2022/06
9. Performing Organization Name and Address Joint Transportation Research Program Hall for Discovery and Learning Research (DLR), Suite 204 207 S. Martin Jischke Drive West Lafayette, IN 47907		**10. Work Unit No.** **11. Contract or Grant No.** SPR-4335
12. Sponsoring Agency Name and Address Indiana Department of Transportation (SPR) State Office Building 100 North Senate Avenue Indianapolis, IN 46204		**13. Type of Report and Period Covered** Final Report **14. Sponsoring Agency Code**
15. Supplementary Notes Conducted in cooperation with the U.S. Department of Transportation, Federal Highway Administration.		

16. Abstract

Environmental conditions is an important factor influencing asphalt pavement performance. The addition of modifiers, both to the asphalt binder and the asphalt mixture, has attracted considerable attention in potentially alleviating environmentally-induced pavement performance issues. Although many solutions have been developed, and some have been deployed, many asphalt pavements continue to prematurely fail due to environmental loading. The research reported herein investigates the synthetization and characterization of biobased phase change materials (PCMs) and inclusion of microencapsulated PCM (μPCM) in asphalt binders and mixtures to help reduce environmental damage to asphalt pavements. In general, PCM substances are formulated to absorb and release thermal energy as the material liquifies and solidifies, depending on pavement temperature. As a result, PCMs can provide asphalt pavements with thermal energy storage capacities to reduce the impacts of drastic ambient temperature scenarios and minimize the appearance of critical temperatures within the pavement structure. By modifying asphalt pavement materials with PCMs, it may be possible to "tune" the pavement to the environment.

17. Key Words asphalt pavements, phase change materials, chemical properties, thermal properties, mechanical properties	**18. Distribution Statement** No restrictions. This document is available through the National Technical Information Service, Springfield, VA 22161.

19. Security Classif. (of this report) Unclassified	**20. Security Classif. (of this page)** Unclassified	**21. No. of Pages** 52 including appendices	**22. Price**

Form DOT F 1700.7 (8-72) Reproduction of completed page authorized

EXECUTIVE SUMMARY

Introduction

Asphalt pavements experience many different diurnal and seasonal temperature fluctuations, which cause the development of thermal stresses in their structures throughout their life cycles. Thus, to maximize pavement performance in such unpredictable environments, asphalt materials must balance the need for thermal management with the need for mechanical resistance. The ability to endow asphalt pavements with thermal energy storage capacities that are based on environmental conditions will enhance the life cycle performance of asphalt pavements. Phase change materials (PCMs) have demonstrated ideal characteristics as thermoregulating agents for various engineering applications. Accordingly, this study aimed to investigate the environmental tuning of asphalt pavements using PCMs. The research objectives of this study were fourfold: (1) investigate the synthesis and characterization of biobased fatty acid amides (FAAms) obtained by direct amidation of different vegetable oils with primary alkyl amines, (2) evaluate the capability of microencapsulated PCM (μPCM) to withstand the mixing and compression stages of the asphalt mixture processing, (3) identify testing techniques that characterize the thermomechanical performance of μPCM-modified asphalt binders and mixtures, and (4) redesign an asphalt mixture with μPCM and determine the mechanical performance implications of incorporating a significant portion of μPCM in the mixture.

Findings

Overall, this study strengthens the concept that modifying asphalt materials with PCMs makes it possible to "tune" the resulting asphalt pavement to the environment, thereby mitigating or eliminating pavement damage due to the exposure of asphalt pavement surfaces to temperature fluctuations. Moreover, although this study focuses on paving applications, the findings may well influence the general synthesis and characterization of PCMs. The following are key findings drawn from this investigation.

- The synthesis of FAAms from different commercial vegetable oils and primary alkyl-amines is feasible, and their chemical and thermal properties are of interest for asphalt paving purposes. Based on green chemistry metrics focused on maximizing resources, the synthesized materials have the potential to be used as PCMs.
- Experimental results suggest that nearly 90% of μPCM particles can survive abrasive forces at room temperature. Additionally, thermal stability tests and image analysis indicate that μPCM particles are stable at asphalt production temperatures (between 135°C–162°C, or 275°F–325°F). However, the combined effects of mixing temperatures and abrasive forces are still a concern and are subject to future investigations.
- Rheological measurements can help identify the latent heat effect of μPCM particles in asphalt binders. This study proposes a novel parameter to determine the temperatures at which the μPCM effect occurs. This approach can also provide insights into the intensity of the μPCM impact on asphalt mixtures.
- The experimental results confirm that μPCM modified asphalt mixture specimens can experience temperature differences between 1.8°C and 10.3°C lower than non-μPCM modified asphalt mixture specimens subjected to the same ambient temperatures.
- The asphalt binder and mixture mechanical test results suggest ambivalent performance outcomes caused by the incorporation of μPCM in asphalt paving materials. However, taken together, the mechanical analysis indicates that the μPCM particles could behave like a conventional mineral filler if they suffer no damage during mixing and compaction.

Implementation

This research demonstrates that the environmental tuning of asphalt materials using PCM could potentially mitigate the appearance of intense surface and inner temperatures on asphalt pavements. This PCM effect promises to improve pavement performance and help alleviate the urban heat island effect. However, the findings of this study suggest that the implementation of PCM modified asphalt pavements in Indiana is currently impractical. The following aspects of this study that could lead to implementing this technology are highlighted below.

- Future work is needed to ensure that PCM modified materials could be readily implemented in the field. More research is required to evaluate the survivability of μPCM during the production, placement, and compaction of asphalt materials. In addition, the long-term performance of the μPCM particles under repetitive vehicle loading and temperature fluctuations must be assessed.
- The technical and environmental improvements generated by the production of biobased PCMs warrant further investigations. Continued efforts will be vital for the large-scale production of biobased PCMs, such as FAAms.
- Chemical, thermal, and visual techniques could be deployed for the characterization of PCMs. These testing techniques show promise at instilling confidence in quality requirements for the production and placement of PCM modified asphalt pavements.
- A proper mixture design procedure that facilitates the incorporation of μPCM in asphalt mixtures has to be established. The framework provided by this study must be refined to modify asphalt mixtures with PCM microparticles.
- This research adds to the modification of asphalt pavements with PCMs and recommends close monitoring of emerging technologies that could help with the temperature management of pavements or any other highway infrastructures asset.

CONTENTS

LIST OF TABLES

LIST OF FIGURES

1. INTRODUCTION

1.1 Background

In recent years, the asphalt pavement industry has recognized the need for designing and constructing roadways that satisfy the requirements of macro and global trends, such as the connectivity, automation, and electrification of road transportation services, as well as conservation of raw materials, climate change, and demographic shifts (Asphalt Institute Foundation, 2017; Kodippily et al., 2018; Mallick et al., 2014). As a result, the advancement of pavement engineering will require the utmost care and the use of state-of-the-art technology. The importance of adequate design provisions to mitigate the effect of environmental conditions on pavement performance cannot be overemphasized (Papagiannakis & Masad, 2008). Asphalt binder viscoelastic properties determine the thermomechanical behavior of asphalt pavements. The binders have a complex chemical composition that exhibits both viscous and elastic properties, depending on temperature and loading time. The exposure of asphalt pavements to normal temperature fluctuations can result in pavement failures. For instance, pavement rutting typically occurs during high temperatures, when the binder stiffness is reduced, while thermal cracking is related to pavement contraction at low temperatures (Behnood et al., 2016; Ray et al., 2009).

The ability of phase change materials (PCMs) to maintain specific temperatures for extended periods can help tune the service temperature of asphalt pavements. The modification of asphalt pavements with PCMs can provide desired engineering properties, such as increased shear modulus and reduced plastic flow at high and intermediate temperatures, and increased resistance to thermal cracking at low temperatures (Kakar et al., 2019a; Kakar et al., 2019b; Refaa et al., 2018; Wei et al., 2019). The advent of PCMs to modify asphalt pavements can be a significant breakthrough for asphalt pavement performance. However, before the large-scale application of this technology, it is necessary to address numerous research and development stages (Sharma et al., 2009). The field implementation of PCM for paving purposes will depend on their environmental, economic, and technical sustainability. Hence, synthetization of PCM from biomass is highly encouraged (Betancourt-Jimenez et al., 2020). Additionally, an in-depth understanding of the effects of PCM on the thermal and mechanical performance of asphalt binders and mixtures is still required. The continued existence of these needs is likely to limit the application of PCMs as asphalt pavement modifiers, despite the potential advantages of their use.

1.2 Motivation

PCM has been extensively investigated as a thermoregulator for various engineering applications, including electronics, spacecraft, solar energy, textiles, buildings, and construction materials, to name a few (Agyenim et al., 2010). Accordingly, the research studies about PCM available in the literature are quantitatively vast. Regarding time, thermal energy storage (TES) started to receive increased attention in the 1970s (Lane, 2018). Thus, most of the information on PCM has been reported over the past 40 years (Zalba et al., 2003). In the literature, the *PCM* term is widely used to refer to a substance that absorbs or releases thermal energy when it undergoes a phase change from solid to liquid, liquid to gas, or vice versa (Dutil et al., 2011). The primary purpose of PCM is the storage of thermal energy in a latent form (Baetens et al., 2010). It is well known that latent heat storage can be achieved through changes in the state of matter (Lane, 2018). If PCM changes from solid to liquid (i.e., liquification, melting) or from liquid to vapor (vaporization, evaporation, boiling), a given system's latent energy increases. Conversely, if the phase change is from vapor to liquid (condensation) or from liquid to solid (i.e., solidification, crystallization), a given system's latent energy decreases. If no phase change is occurring, there is no change in latent energy (Incropera, 2007). Therefore, a proper understanding of the fundamental concepts and principles that underlie PCM incorporation to any system is required for its optimization (Oró et al., 2012).

In general, the incorporation of PCMs into asphalt pavements has been inspired by the successful application of PCMs in a wide variety of engineering fields. The challenges currently faced by asphalt pavement scholars to understand this topic overlap with the obstacles experienced by scholars in other engineering disciplines. Several approaches could be used for the proper selection and optimization of PCM for asphalt pavement purposes. A fundamental understanding of PCM's latent heat storage capacity is essential to promote PCM modified asphalt pavements.

More specifically, this research study was primarily motivated by previous work done by the authors. Montoya et al. (2021) demonstrated through experimental and computational results that PCM can assist in preventing the snow accumulation and ice formation in the surface of asphalt pavements and delay the appearance of freezing temperatures across the pavement's depth. The computational approach presented by Montoya et al. (2021) was extended to predict the effectiveness of PCM modified asphalt pavements in the state of Indiana, as shown in Figure 1.1. The PCM effectiveness parameter represents the percentual reduction of time experienced by the pavement below 0°C (32°F) when modified with PCM and relative to a reference pavement without PCM.

The PCM effectiveness values were calculated by modeling asphalt pavement slabs with and without PCM and subjecting them to realistic ambient temperature data from 20 locations in Indiana. The climatic data gathered consisted of hourly temperature averages recorded from May 2019 to April 2020. The heat transfer simulations suggested that if a 76.2-mm (3-in.) asphalt pavement slab was modified with about 11% of PCM by total pavement slab volume,

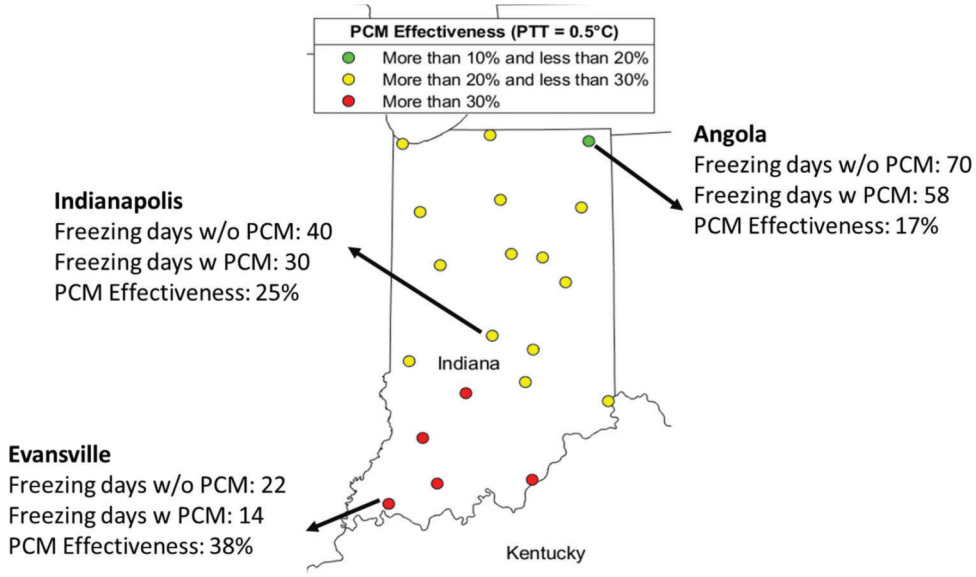

Figure 1.1 PCM effectiveness in Indiana based on computational analysis.

pavements in Indiana could experience a yearly reduction in freezing times between approximately 5% and 42%. These computational results provided strong support for the environmental tuning of asphalt pavements using PCM. However, this preliminary analysis was demonstrated by incorporating the PCM into the pavement slabs using steel pipes embedded in the pavement structure. The steel pipes contained the PCM substances applied for thermal management. Embedding pipes in the PCM modified asphalt pavement slab was ideal for prototyping and gaining knowledge about this methodology, but it is impractical for scaling implementation. A much more pragmatic approach should be developed to propose the large-scale and long-term application of PCM modified asphalt pavements.

Additionally, the PCM effectiveness values reported in Figure 1.1 correspond to a PCM with a phase temperature transition (PTT) of 0.5°C. As can be seen in Table 1.1, the PCM effectiveness averages across all locations when the PTT were 0.5°C, 1.5°C, 2.5°C, and 3.5°C were equivalent to 26.6%, 23.6%, 16.5%, and 10.7%, respectively. The evidence indicated that as the PTT departed from 0°C, the PCM effectiveness decreased at all locations. The commercially available fatty acid methyl esters used in the experimental work done by Montoya et al. (2021) had PTT between 2.0°C and 3.5°C. Thus, the PCM effectiveness depends on the production of PCM substances that absorb and release latent heat energy at suitable temperature ranges to delay the appearance of specific undesirable temperatures in the pavement structure. Additionally, PCMs should be produced from abundant and inexpensive resources rather than from scarcer and more expensive raw materials (Betancourt-Jimenez et al., 2020). As a result, this project aimed to contribute to these growing research areas by exploring the synthetization of environmentally friendly PCMs and the systematic inclusion of PCMs to asphalt binders and mixtures using microencapsulated PCM (μPCM).

1.3 Research Objectives

By modifying asphalt materials with PCM, it should be possible to "tune" the resulting asphalt pavement to the environment, thereby mitigating or eliminating pavement damage due to the exposure of asphalt pavement surfaces to temperature fluctuations. Accordingly, the research objectives of this study were fourfold: (1) investigate the synthesis and characterization of biobased PCMs obtained by direct amidation of different vegetable oils with primary alkyl amines, (2) evaluate the capability of μPCM to withstand the mixing and compression stages of asphalt mixture processing, (3) identify testing techniques that characterize the thermomechanical performance of μPCM modified asphalt binders and mixtures, and (4) redesign an asphalt mixture with μPCM and determine the mechanical performance implications of incorporating a significant portion of μPCM in the mixture. These objectives were identified as critical to addressing the research gaps associated with the large-scale implementation of PCM modified asphalt pavements. Therefore, a series of experimental procedures are demonstrated, the results of which can be instrumental in extending the knowledge of PCM modified asphalt pavements.

1.4 Organization of the Report

The report consists of six chapters, and it is organized to elaborate on the research objectives outlined above individually. This first chapter introduces the background, motivation, and research objectives for this study. The second chapter examines the feasibility of synthesizing biobased FAAms for PCM applications. The third chapter presents experiments that

TABLE 1.1
PCM effectiveness at 20 locations in Indiana

	Number of Locations			
	PCM Phase Transition Temperature (°C)			
PCM Effectiveness (%)	**0.5**	**1.5**	**2.5**	**3.5**
≤10	0	0	1	10
>10 and ≤20	1	7	15	10
>20 and ≤30	14	10	4	0
>30	5	3	0	0
	PCM Effectiveness (%)			
Average Across All Locations	26.6	23.6	16.5	10.7

evaluate the resistance of μPCM for paving purposes. The fourth chapter attempts to capture the μPCM effect in asphalt binders and mixtures. The fifth chapter demonstrates the redesign of an asphalt mixture with μPCM and evaluates its mechanical performance. The sixth or final chapter provides conclusions and recommendations derived from this research.

2. SYNTHESIS AND CHARACTERIZATION OF BIOBASED FATTY ACID AMIDES

2.1 Background

As mentioned in the previous chapter, PCMs consist of substances that absorb significant amounts of energy when they melt and release it back to their surroundings when they solidify (Fleischer, 2015). These substances are usually classified as organic or inorganic, with the former the most used due to their high thermal cycling stability, low degree of supercooling, non-corrosiveness, and low cost (Behzadi & Farid, 2014). However, these are generally derived from petroleum, which constitutes an issue from the environmental standpoint. Some efforts have been done to obtain PCM from renewable sources (Aydin & Aydin, 2012; Floros & Narine, 2016; Naresh et al., 2020; O'Neil et al., 2019; Raghunanan et al., 2016; Ravotti et al., 2018), but their production often involves carrying out complex chemical reactions, low yields, or a series of fractionation and purification stages that increase the cost of the final product, making it impossible for these biobased PCM alternatives to compete with the unexpensive petroleum-derived paraffins available in the market.

This chapter summarizes the efforts conducted to obtain biobased PCMs from highly abundant vegetable oil feedstocks using a simple, high yield method. Different vegetable oils can be reacted with alkyl amines to obtain fatty acid amides (FAAms) with high latent heats and varying melting temperatures, making them suitable for PCM applications (Betancourt-Jimenez et al., 2020). Due to the simplicity and the high yield of the synthesis process, unexpensive nature of the reactants, and ease of purification, this method could be scaled to industrially produce cheap biobased PCMs with a small environmental footprint.

2.2 Methods

2.2.1 Synthesis of Fatty Acid Amides

Twelve different FAAms were synthesized, each from one vegetable oil (corn, sunflower, or palm oil) and one alkylamine (butylamine, octylamine, dodecylamine, or hexadecylamine). Briefly, 4.0 g of oil (~14 mmol) were reacted with three times molar excess amine (~126 mmol) and 20 mg of DABCO (~0.2 mmol). The reaction was carried out at 60°C during 72 hours with magnetic stirring. The purification step varied depending on the amine used during synthesis; for FAAms synthesized from butylamine or octylamine, the product was rinsed twice with deionized water and recovered using a separatory funnel. Lastly, the product was subjected to high vacuum until the pressure stabilized (approximately at 300 mTorr) to evaporate any remaining water and unreacted amine. In the case of FAAms synthesized from dodecylamine or hexadecylamine, the product was dissolved in ethanol (20 ml/g), recrystallized at –10°C and 0°C, respectively, and vacuum filtered to remove the ethanol with the unreacted amine and byproducts. This process was repeated twice. Next, the purified product was dried in a vacuum oven at 100°C for 2 hours to remove any remaining ethanol.

Oils are typically a combination of different triglycerides which are esters that consist of a glycerol molecule bound to three fatty acid molecules (Dickinson & McClements, 1996). The specific fatty acid composition of the triglycerides in the oils used in this work was initially unknown, however, compositions found in literature are shown in Table 2.1 and were used as a reference to estimate the molecular weight of the oils and resulting FAAms.

2.2.2 Characterization of Fatty Acid Amides

The chemical composition of the obtained FAAms was analyzed through Fourier Transform Infrared (FT-IR) using an Attenuated Total Reflection (ATR) accessory with a Spectrum Q100 Spectrometer (Perkin Elmer). Each analysis was conducted in a 4,000–600 cm^{-1} wavelength range under 10 scans. The background

TABLE 2.1
Fatty acids contents for corn oil, sunflower oil, and palm oil (Flagella et al., 2002; Rohman & Che Man, 2012; Zambiazi et al., 2007)

	Fatty Acid Content (wt.%)						
	Literature Values				Experimental Values		
	Saturated		Unsaturated		Saturated	Unsaturated	
Oil	C16:0	C18:0	C18:1	C18:2	C16:0+C18:0	C18:1	C18:2
Corn Oil	12.7	2	27.5	53.2	15	30.2	54.8
Sunflower Oil	3.2	4.4	83.3	7	7.6	73.5	18.9
Palm Oil	42.7	4.6	39.4	10.6	55.4	35.9	8.7

Note: Palmitic acid (C16:0), stearic acid (C18:0), oleic acid (C18:1), and linoleic acid (C18:2).

signal was subtracted, and the baseline was flattened for all the spectra. Nuclear Magnetic Resonance (NMR) spectroscopy was also conducted to further study the chemical composition of the FAAms. Each FAAm was dissolved in deuterated-chloroform and analyzed using a Bruker AV-III-400-HD spectrometer. The instrument is equipped with a 5-mm BBFO Z-gradient probe. Analysis was conducted at 400 Hz, and 8 and 512 scans for ^{1}H and ^{13}C (i.e., hydrogen and carbon), respectively. Additionally, the melting and crystallization temperatures along with latent heats for both transitions were determined using Q2000 Differential Scanning Calorimetry (DSC) analyzer (TA Instruments). Heating and cooling rates were 10°C/min and analysis was conducted over a –100°C to 100°C temperature range in a nitrogen atmosphere. The thermal stability of the FAAms was assessed using a 50Q Thermogravimetric Analyzer (TGA) from TA Instruments. For this, each sample was ramped at 15°C/min from room temperature to 600°C in a nitrogen atmosphere.

2.2.3 Green Chemistry Metrics of Fatty Acid Amides

The sustainability of the synthesis process was assessed using different metrics widely accepted in the scientific community such as Atom Economy (AE), the Environmental Factor or E Factor (EF) and the EcoScale (Constable et al., 2002; Dicks & Hent, 2015). In the case of the environmental factor, two different parameters proposed by Roschangar et al. (2015) were calculated, the Simple E Factor (sEF) and the Complete E Factor (cEF).

2.3 Deliverables

2.3.1 Fatty Acid Amides Synthesis

The synthesis method used in this work was previously reported by Bilyk et al. (1992). This reaction is carried out without the addition of organic solvents, in the presence of oxygen, at room pressure and with mild heating (60°C). The mechanism starts by the nucleophilic attack of the catalyst on the carbonyl of the glyceride, causing the displacement of the alkoxide and formation of the alcohol by addition of a proton from the media. Subsequent nucleophilic attack of the cationic quaternary amide by the primary alkyl amine displaces and reforms the catalyst. Since alkoxide is known to be a poor leaving group (Bilyk et al., 1992), three times molar excess amine and mild heating were used to increase the conversion rate. While this amount of excess is not feasible at scale, the purpose was to synthesize enough FAAm at a high enough purity to test thermal response, not to optimize the reaction. In this work, DABCO was chosen as catalyst due to its eco-friendly nature, low toxicity, and high reactivity (Yang et al., 2008).

Three oils and four amines were used to synthesize a total of 12 different FAAms. Due to differences in fatty acid composition (Table 2.1), FAAms from each oil are expected to exhibit different thermal properties. The amines used had 4, 8, 12, and 16 carbon chains in their backbones, respectively. These amines were chosen to study the effect of hydrocarbon length in the transition temperatures and latent heats of the resulting amides. The purification step varied depending on the reactants used for synthesis since higher molecular weight amines (dodecylamine and hexadecylamine) are not water-soluble and water rinsing was not an effective approach for their removal. Conversely, ethanol rinsing was not suitable for FAAms from amines with lower molecular weights (butylamine and octylamine) since the recrystallization temperatures of those were too low.

The molecular weight of the resulting FAAms were estimated from the oil compositions presented in Table 2.1 and the molecular weight of the amines used. The theoretical weight of FAAms were determined based on the amount of oil used for synthesis and full conversion of this reactant was assumed. Equation 2.1 was then used to calculate the yield of each reaction relative to the oil and results are listed on Table 2.2.

$$Yield(\%) = \frac{W_P}{W_T} \times 100 \qquad \text{(Equation 2.1)}$$

where W_P corresponds to the amount of FAAm recovered after purification and W_T is the theoretical amount of synthesized FAAm. The yield for each FAAm was above 70%, which is high considering that part of the product was lost during purification. It must be noted that in some cases partial solidification of the products was observed before the reaction ended. For this reason, it is believed that the synthesis could have

TABLE 2.2
Reaction yields after purification

Oil	Amine	Yield (%)
Corn Oil	Butylamine	70
	Octylamine	85
	Dodecylamine	72
	Hexadecylamine	78
Sunflower Oil	Butylamine	77
	Octylamine	81
	Dodecylamine	74
	Hexadecylamine	81
Palm Oil	Butylamine	80
	Octylamine	83
	Dodecylamine	70
	Hexadecylamine	83

been completed in less than 72 hours, especially for FAAms where longer amines were used. This theory is based on the work of Bilyk et al. (1992) where shorter reaction times were observed for higher molecular weight amines. Nonetheless, the effect of reaction time on yield was not studied and is recommended for future work.

2.3.2 Chemical Characterization

Figure 2.1 shows the FTIR spectra of corn oil and its FAAms derivatives. In the corn oil spectrum, the stretching of the =C-H bonds (in linoleic and oleic segments) and the C-H bonds (in methylene groups) are observed around 3,010 and 2,900–2,800 cm^{-1}, correspondently. Also, bands associated to the stretching of both the C=O and C-O bonds in the ester groups are found around 1,744 and 1,160 cm^{-1}, respectively. Lastly, bands corresponding to the scissoring and rocking of methylene groups are observed at 1,460 and 722 cm^{-1} (Rohman & Che Man, 2012; Safar et al., 1994).

The conversion of corn oil to FAAms is confirmed by the appearance of the N–H stretching band of the amide group at 3,300 cm^{-1}. Also, the C=O stretching band shifted to lower frequencies (around 1,630 cm^{-1} instead of 1,744 cm^{-1}) due to the presence of the amide group. New bands are also found around 1,550 and 690 cm^{-1}, caused by N–H bending and N–H wagging, respectively. It can also be noted that the C–O stretching band of the ester group is not present in any spectra of the FAAms, confirming once more the successful synthesis of the amide.

Since all the FAAms from corn oil have the same functional groups in their chemical structures, their spectra were very similar despite being synthesized from different amines. However, when longer amines were used, more methylene units were introduced into the chemical structure of the resulting FAAms, reducing the ratio of amide to methylene groups and decreasing the intensity of the signals of N–H, and C=O vibrations.

As seen in Figures A.1 and A.2 in the Appendix A, the FT-IR spectra of both sunflower and palm oils

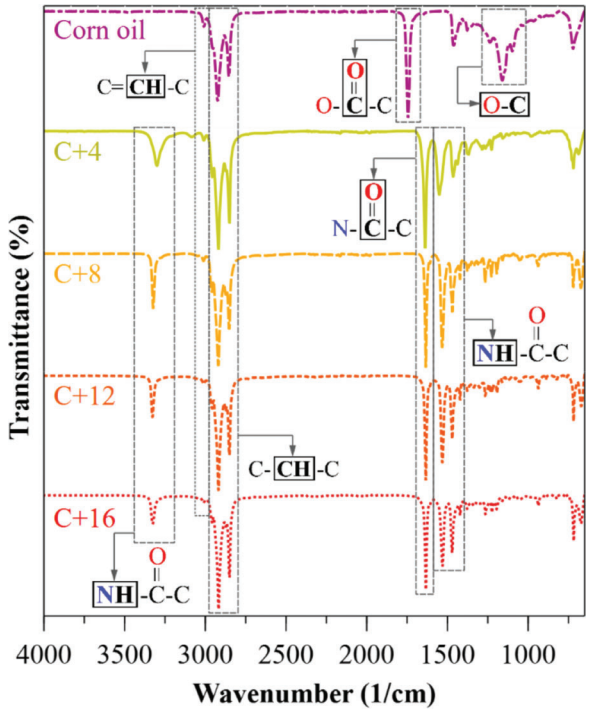

Figure 2.1 FT-IR spectra of pure corn oil and fatty acid amides (FAAms) from corn oil and butylamine (C+4), corn oil and octylamine (C+8), corn oil and dodecylamine (C+12), and corn oil and hexadecylamine (C+16).

show most of the characteristic bands observed for corn oil since they all have similar chemical structures. The only significant difference is the absence of the =C–H stretching band for palm oil (~ 3,010 cm^{-1}), which is explained by the decreased amount of unsaturated bonds contained in its structure. Conversion of sunflower oil and palm oil to FAAms was also evidenced from FTIR analysis.

^{13}C NMR spectra of pure corn oil along with its FAAms derivatives are shown in Figure 2.2. The peaks at 173 ppm corresponds to carbons in the carbonyl groups of the triglycerides. The series of peaks found in the 125–135 ppm region appear as a result of the carbon-carbon double bonds found in the oleic and linoleic segments. Peaks at 69 ppm and 62 ppm correspond to carbons forming the ester groups. The peak found around 34 ppm corresponds to carbons adjacent to the carbonyl group in the ester. Lastly, peaks found in the 32–10 ppm region correspond to methyl and methylene groups (Burrows et al., 2013).

^{13}C NMR spectra of the FAAms from corn oil and the amines are very similar and they show two main differences when compared to pure corn oil. First, no peaks in the 55–70 ppm region are found, indicating that no ester groups exist in the chemical structure of the synthesized FAAms. Second, new peaks are found around 39 ppm and 37 ppm, which corresponds to carbon bonded to nitrogen atoms and carbon adjacent to carbonyl groups in the amide group, respectively. Also, the height of the peaks resulting from both carbon-carbon double bonds and the amide group

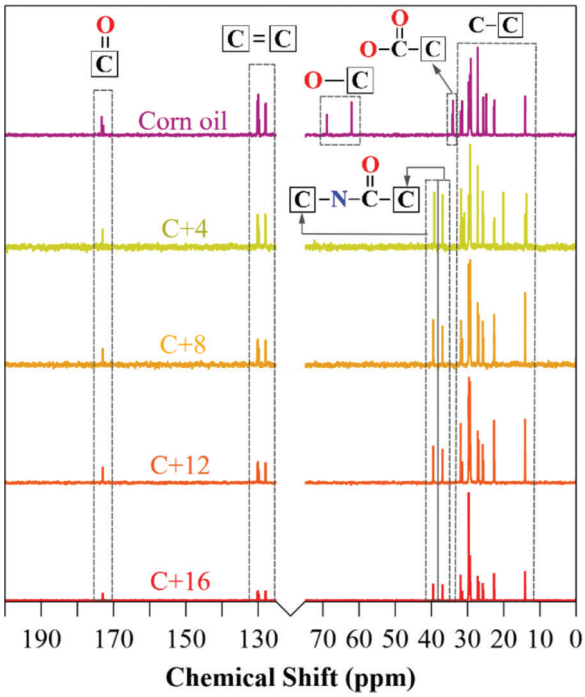

Figure 2.2 ^{13}C NMR spectra of corn oil and fatty acid amides from corn oil and butylamine (C+4), corn oil and octylamine (C+8), corn oil and dodecylamine (C+12), and corn oil and hexadecylamine (C+16).

decrease as the precursor amine gets longer, which results from the introduction of a larger number of methylene groups into the structure.

^{13}C NMR results for sunflower oil, palm oil, and their FAAms derivatives are presented in Figures A.3 and A.4 (see Appendix A), respectively. Both spectra presented the same characteristic peaks observed for corn oil with some variations in their magnitudes which are attributed to differences in their triglyceride profiles (see Table 2.1). The spectra of FAAms from palm oil and sunflower oil corroborate once more the full conversion of the triglycerides into amides.

^{1}H NMR was also conducted, and the spectra of the samples are presented in Figures A.5–A.8 (see Appendix A). The fatty acid profiles of the oils and their FAAms were determined by integrating the signals in the spectra. The experimentally determined fatty acid compositions of the oils are very similar to those reported in the literature (see Table 2.1). Small differences exist which are to be expected considering factors such as sowing date, water regime, growing location and climate conditions have an influence on the oil composition (Flagella et al., 2002; Lajara et al., 1990). Also, small variations in the integration values of the ^{1}H NMR signals can significantly affect the fatty acid profile obtained, introducing an error in the measurements (Knothe & Kenar, 2004).

The composition of each FAAm was also determined to ensure that the initial proportion of the fatty acids was maintained after the synthesis reaction. Results presented in Table 2.3 show slight changes in the fatty acid profile of the FAAms depending on the precursor amine used. Nonetheless, no trends could indicate that any amine is more likely to react with a specific fatty acid segment. Hence, differences in composition are believed to have been introduced during the purification process.

2.3.3 Thermal Characterization

Thermal properties of the as-purchased corn, sunflower, and palm oils were assessed through DSC and their respective thermograms are presented in Figure 2.3. As it can be noted in the plot, each oil exhibited very different thermal profiles. In the case of corn oil, two broad overlapping peaks are observed for both crystallization and melting transitions. The presence of multiple peaks in oils is attributed to their complex composition consisting of a mixture of numerous triglycerides with different fatty acid segments. Generally, triglycerides with a higher content of saturated acids melt and crystallize at higher temperatures than triglycerides richer in the unsaturated versions (Pardauil et al., 2017).

The behavior observed for sunflower oil was quite different, exhibiting only one peak for both crystallization and melting transitions. This behavior has been reported before for highly unsaturated oils and indicates that the different triglycerides interact with each other during the cooling process and are able to co-crystallize into the same structure. This is possible due to the similarity of the triglyceride components, which for sunflower oil are mostly oleic and linoleic acid (Tan & Che Man, 2002). The small exothermic peak found right before the melting transition indicates that some recrystallization took place during the heating step of the experiment. Due to their polymorphic nature, triglycerides can form different crystalline structures depending on several factors including the nature of the fatty acid segments, the purity of the sample and the crystallization procedure (Lavigne et al., 1993). It has been reported (Tan & Che Man, 2002) that when oil samples are heated, some triglycerides can rearrange and recrystallize

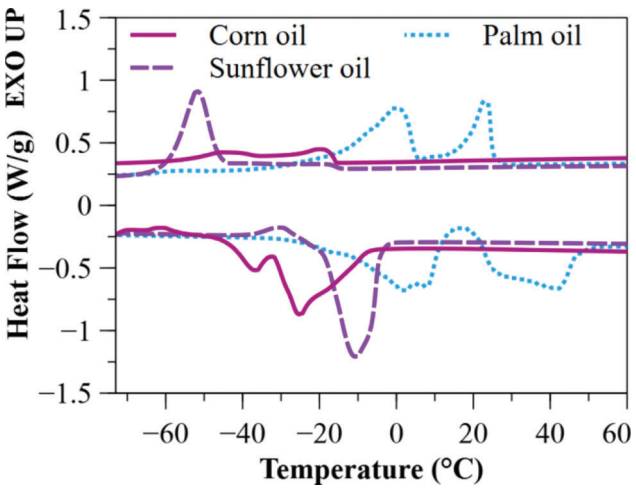

Figure 2.3 DSC diagram of corn, sunflower, and palm oils.

TABLE 2.3
Experimentally determined fatty acid composition (wt.%) of the FAAms

Oil	Amine	FAAm from Saturated	FAAm from Unsaturated	
		C16:0 + C18:0	C18:1	C18:2
Corn Oil	Butylamine	10.8	30.7	58.5
	Octylamine	14.8	33.4	51.8
	Dodecylamine	18.2	32.0	49.0
	Hexadecylamine	14.6	30.7	54.7
Sunflower Oil	Butylamine	6.7	72.3	21.0
	Octylamine	7.0	73.4	19.7
	Dodecylamine	9.6	76.6	13.8
	Hexadecylamine	7.3	75.4	17.4
Palm Oil	Butylamine	54.8	33.9	11.3
	Octylamine	55.3	35.4	9.3
	Dodecylamine	64.3	30.9	4.9
	Hexadecylamine	59.0	34.9	6.0

TABLE 2.4
Latent heat of melting and crystallization for corn oil, sunflower oil, palm oil, and their FAAm derivatives

Material	T_m (°C)	$\Delta H_{melting}$ (J/g)	T_c (°C)	$\Delta H_{crystallization}$ (J/g)
Corn Oil	–24.6 ± 0.3	52 ± 1	–22 ± 1	52 ± 1
C+4	7.8 ± 0.1	94 ± 3	2.6 ± 0.1	94.1 ± 0.2
C+8	25.6 ± 0.2	114.5 ± 0.8	20.6 ± 0.1	112 ± 1
C+12	46.0 ± 0.1	128.5 ± 0.6	38.0 ± 0.1	123 ± 1
C+16	59.8 ± 0.2	125.3 ± 0.9	53.5 ± 0.2	123.0 ± 0.9
Sunflower Oil	–9.8 ± 0.2	61 ± 1	–44.8 ± 0.1	57.5 ± 0.4
S+4	21.5 ± 0.2	106 ± 1	10.5 ± 0.4	100 ± 1
S+8	30.1 ± 0.1	117.8 ± 0.7	22.0 ± 0.3	117.6 ± 0.2
S+12	49.3 ± 0.2	139.5 ± 0.9	37 ± 1	136.8 ± 0.9
S+16	61.7 ± 0.1	126.6 ± 0.3	55.8 ± 0.1	125.8 ± 0.2
Palm Oil[1]	1.5 ± 0.1, 26.8 ± 0.6	76 ± 1	0.9 ± 0.1, 23.2 ± 0.6	66 ± 1
P+4[1]	19.2 ± 0.2, 58.3 ± 0.1	100 ± 2	13.6 ± 0.1, 51.5 ± 0.5	95.5 ± 0.9
P+8[1]	31.6 ± 0.1, 61.4 ± 0.1	136 ± 1	24.2 ± 0.1, 51.2 ± 0.1	134 ± 1
P+12[1]	47 ± 1, 69.4 ± 0.2	141 ± 3	40.1 ± 0.1, 64.0 ± 0.2	127 ± 2
P+16[1]	60.1±0.1, 83.1±0.1	133 ± 2	53.5 ± 0.3, 78.1 ± 0.2	132 ± 1

Note:
FAAms from C = corn oil, S = sunflower oil, P = palm oil, 4 = butylamine, 8 = octylamine, 12 = dodecylamine, 16 = hexadecylamine.
[1]Two transitions are observed for both cooling and heating.

in more stable polymorphs which appears as an exotherm in the heating curve of the DSC thermogram.

For palm oil, two exotherms were obtained after cooling the sample from the melt. This was expected since approximately 45 wt.% of the sample is rich in unsaturated acids (linoleic and oleic) (refer to Table 2.1) that crystallize at lower temperatures, while the other triglycerides are mainly made of saturated segments (palmitic and stearic) and typically exhibit higher crystallization temperatures. The high content of both types of triglycerides and their marked difference in degree of saturation makes it unlikely for them to interact and co-crystallize into the same structure, hence producing more than one peak upon cooling.

Based on the previous discussion of their thermal properties none of the as-received oils exhibit the right characteristics to be used as PCMs. The latent heat (ΔH) of melting and crystallization for each of these oils is around 52–76 J/g (see Table 2.4), which is lower than those of commercial organic PCMs usually ranging between 86–340 J/g (Zalba et al., 2003). Additionally, they are prone to exhibit polymorphism, and they melt and crystallize over wide temperature ranges, making them unsuitable materials for thermal management applications.

As it can be seen in Figure 2.4(a), the thermal properties of corn oil drastically change after reaction with any of the amines. The most significant difference is that some of the obtained FAAms exhibit only one

peak for each transition. Additionally, all FAAms melt and solidify over narrow temperature ranges when compared to corn oil. The two FAAms that did not show single peaks were the ones synthesized from butylamine and dodecylamine. However, the FAAm from dodecylamine shows one large peak overlapped with a small one upon cooling and the temperature range in which this amide crystallizes might still be narrow enough to be considered a good candidate for PCM applications. Note that all DSC experiments were conducted at high cooling and heating rates (10°C/min), which are known for broadening the peaks and shifting them to lower temperatures in cooling and to higher temperatures in melting (Cebula & Smith, 1991). This effect worsens in materials with poor thermal conductivities; hence it is possible that these FAAms exhibit sharper peaks at lower rates. However, the effect of cooling and heating rates on the thermal behavior of the FAAms is out of the scope of this work.

The appearance of single peaks in some corn oil derived FAAms is remarkable considering that these materials consist of a mixture of amides derived mostly from triglycerides of oleic, linoleic and palmitic acids. Results shown in Figure 2.4(a) suggest that even though these amides have different chemical structures, they interact with each other and either solidified into the same crystalline structure or into several crystalline structures with similar melting points. Possible factors that could be promoting co-crystallization is that despite their differences, these FAAms have similar numbers of methylene units in their structures (C16 or C18), are linear, and the ratio of $-CH_2$ groups to unsaturations and amide groups is large. Also, it is possible that hydrogen-bonding of the amide group diminishes the role that unsaturation differences play during crystallization, making the amides pack in similar ways. Nonetheless, it is believed that the ratio of $-CH_2$ groups to unsaturations and amide groups dominates over hydrogen bonding interactions. FAAms from butylamine which have the smaller number of methylene groups in their structures, were the only ones to exhibit three individual crystallization events upon cooling. A possible explanation is that unsaturations are not as "diluted" in the structure of these FAAms and play a more significant role, impeding co-crystallization.

Results also indicate that the proportion of saturated and unsaturated segments in the sample have the larger effect on co-crystallization. As mentioned before, FAAms from dodecylamine exhibited one main peak overlapped by a small one during the cooling segment, a different behavior than that observed for FAAms from octylamine and hexadecylamine. The presence of this small overlapping peak is believed to be caused by the slightly increased concentration of saturated acid segments in the sample, which could be promoting the formation of a new crystal structure at a higher temperature.

Figure 2.4(a) also shows that the melting point of the FAAm increases with the length of the amine used. This was expected since linear organic compounds of the same kind increase their melting points with molecular weight (Stauffer et al., 2008). The magnitude of the peaks (i.e., latent heat) also increases with the molecular weight of the amine, except for the case where hexadecylamine was used (refer to Table 2.4). Latent heat is an inherent property of the molecule and when a first-order transition is taking place is given by Keshavarz et al. (2016) and Mandelkern (2002), as shown in Equation 2.2.

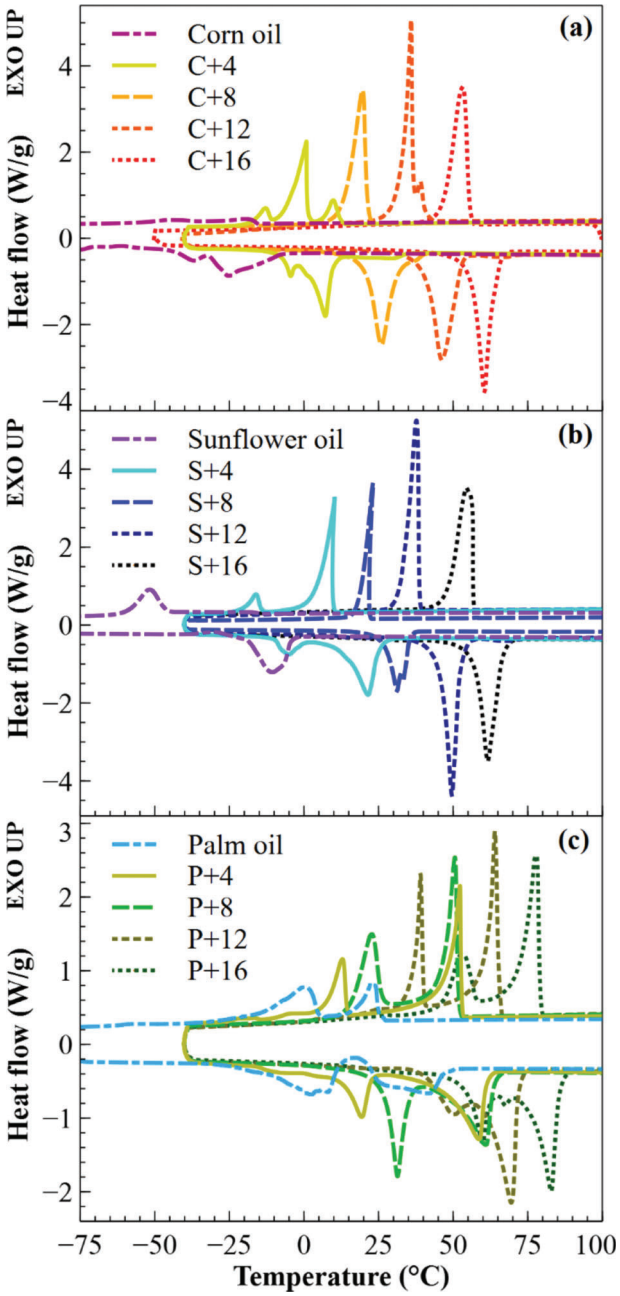

Figure 2.4 DSC diagram of (a) FAAms from corn oil, (b) FAAms from sunflower oil, and (c) FAAms from palm oil. C = corn oil, S = sunflower oil, P = palm oil, 4 = butylamine, 8 = octylamine, 12 = dodecylamine, and 16 = hexadecylamine.

$$\Delta H = T\Delta S \qquad \text{(Equation 2.2)}$$

where ΔH is the enthalpy or latent heat, T is the temperature, and S is the change of entropy associated with the transition. The latent heat of fusion of a substance is directly proportional to its melting point, which explains the continuous increase of latent heat observed for FAAms from butylamine, octylamine, and dodecylamine. However, this is not true for FAAms from hexadecylamine which have the highest melting temperature of all the amides but a lower latent heat than C+12. It is believed that in this case, the entropy of fusion of the C+16 FAAm is significantly lower and this surpasses the effect of having a higher melting point, ultimately causing an overall enthalpy reduction.

Thermal properties of FAAms from sunflower oil were also studied, and the results are presented in Figure 2.4(b). The changes observed in sunflower oil after reaction with the amines are the same reported for corn oil. This was somewhat expected considering that both oils consist mostly of unsaturated fatty acids. It can be stated that increasing the number of methylene groups in the molecule promotes co-crystallization of the FAAms. The most relevant evidence of this is the change in thermal behavior of FAAms synthesized from octylamine, which showed one peak for crystallization and two overlapping peaks for melting in contrast to FAAms from butylamine that presented two distanced peaks in both cases.

The DSC diagrams of FAAms synthesized from palm oil are presented in Figure 2.4(c). All the amides from palm oil exhibited two melting and crystallization peaks instead of one. It must be noted that FAAms from palm oil have high contents of both saturated and unsaturated acid segments (59% and 41%, respectively). It is possible that since both groups were present in similar proportions, segregation during cooling was promoted causing the saturated FAAms to crystallize at higher temperatures, followed later in the process by the unsaturated FAAms at lower temperatures. This segregation was not seen in FAAms from corn and sunflower oils since even when these two groups also existed, their proportions were very different, with unsaturated amides constituting about 75–80 wt.% of the product. In these cases, since the content of saturated FAAms was small, they were "diluted" in the unsaturated amides and interacted with them during the cooling process instead of segregating, making it possible for them to co-crystallize into the same structures.

Except for exhibiting two peaks instead of one, FAAms from palm oil showed the same trends observed for those derived from corn and sunflower oils. Based on results presented in Table 2.4, the two transitions observed in the FAAms from palm oil grow closer by approximately 10°C every time the length of the amine is increased by four methylene units starting at 4 (butylamine) and ending at 12 (dodecylamine). It is possible that as more $-CH_2$ units are introduced into the FAAms, the effect of unsaturations on crystallization becomes less significant and the crystalline structures formed are more similar, shortening the distance between the transitions. However, the effect of increasing the number of methylene units is limited considering that when it is increased from 12 to 16 (hexadecylamine), the distance between the two transitions remains unchanged (around 20°C).

TGA results of the FAAms from the three different oils are shown in Figure 2.5. The diagrams show that the weight of all the FAAms remains constant at temperatures below 200°C (392°F) and that the evaporation temperature increases as the amine used for synthesis gets longer, independently of the precursor oil. The boiling point is directly proportional to molecular weight which explains why the FAAms have higher evaporation temperatures as their length is increased. The FAAms also have higher evaporation temperatures than other PCMs with similar melting points. For example, FAAms from corn oil and butylamine (C+4) which melt around 7°C evaporate about 100°C above methyl laurate, a PCM material with a melting point of 5°C. This feature can be particularly advantageous in applications where the PCM material will be subjected to high temperatures.

2.3.4 Green Chemistry Metrics of Fatty Acid Amides

Results of the atom economy, E factor, and EcoScale are presented in Table 2.5. The %AE results obtained are above 91.7% for all the FAAms, which are high despite the fact their synthesis results from a substitution reaction where byproducts are generated. Fortunately, the molecular weight of glycerol is considerably lower than that of the FAAms, which makes possible that these syntheses present such high values of %AE. Another fact that greatly contributed to the results obtained is that the chosen synthesis route consists of only one step. As mentioned before, high %AEs such as the ones obtained for the FAAms are desired since they indicate low amounts of waste are associated to the reaction's mechanism. Selecting a synthesis route with a high %AE is the first step to design a green organic preparation (Constable et al., 2002; Dicks & Hent, 2015; Sheldon, 2018).

As mentioned in the experimental section, two values of EF were determined to define the lower and upper bounds of the waste generated in the production of the FAAms. Results obtained for the sEF were around 0.61–1.22. It must be noted that these values were significantly affected by two factors: the yield of each reaction and the use of excess reactants in large quantities. The decreased yields obtained for each FAAm are associated to product losses introduced during purification and not to reaction conversion, hence, they can be increased by improving the purification methodology. Additionally, reactants were used up to 3 times in excess to ensure the full conversion of the oils to amides. If these reactions were optimized, their sEF values could be lowered. For example, in the conservative case where the amount of reactants were decreased from 3 to 1.5 times excess and the yield were increased to 90%, the sEF would range from 0.34–0.47, a significant decrease from the current values.

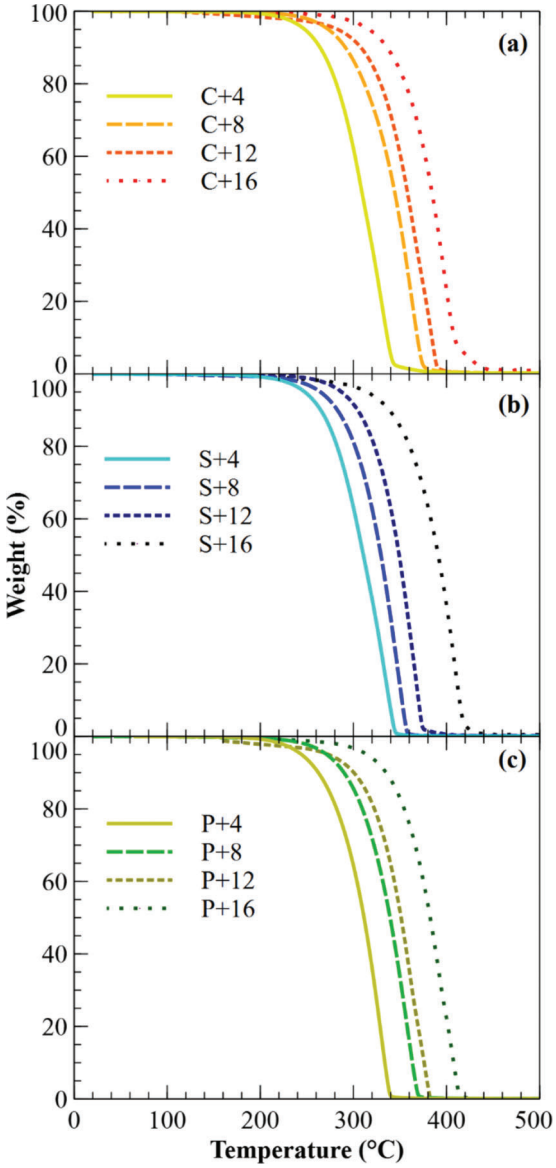

Figure 2.5 TGA diagram of FAAms. (a) FAAms from corn oil, (b) FAAms from sunflower oil, and (c) FAAms from palm oil. C = corn oil, S = sunflower oil, P = palm oil, 4 = butylamine, 8 = octylamine, 12 = dodecylamine, and 16 = hexadecylamine.

The cEF results ranged from 36.20 to 46.49, a notable increase when compared to obtained sEF values. The main difference between these two parameters is that water and ethanol used in the purification steps were included in the calculation of cEF. However, it must be noted that due to differences in the boiling points of ethanol and the reactants and byproducts, the first can be recovered using a rotary evaporator. Recycling the ethanol will significantly lower the real EF of FAAms synthesized from dodecylamine and hexadecylamine, bringing it to values close to those of sEFs.

The biobased PCMs here produced are a potential alternative to petroleum-derived paraffins, a non-renewable source widely known for having an important environmental impact. The environmental factor of paraffins was not found in the literature, nevertheless, values of EF of less than 0.1 have been reported for the oil refining industry (Sheldon, 2018). One possible explanation for such a low EF is that virtually all the byproducts of gasoline production are commercialized for different applications and are not considered waste. An important factor that needs to be accounted for before drawing any conclusions is that EF values reported in this work correspond to a laboratory synthesis that has not been optimized. EF values found in the literature often correspond to highly optimized industrial settings that use sophisticated techniques for solvent recovery and water treatment. This results in waste minimization and translates into very low EF values. Therefore, it would be unfair to compare the EF of oil refining industry to the values here reported. Again, there is plenty of room for optimization of the FAAms production process including decreasing the amount of solvents used in the purification steps or using other purification methods that do not required the use of large amounts of solvents. These changes could drastically lower the EF of FAAms, allowing them to compete with paraffins. Regardless, unlike paraffins which are completely petroleum derived, and therefore depleting, FAAm is partially to totally renewable (depending on the source of amine), which is an inherent improvement in sustainability.

The EcoScale results ranged from 69.0 to 82.5. These high values result from the relative low toxicity of the reactants, low cost of the materials, simplicity of the experimental setup and high yields obtained. Note that these reactions could score even higher EcoScale values if their yields are increased. EcoScale results obtained are encouraging since they shed light on other aspects that contribute to the greenness of this preparation such as the use of inexpensive plant feedstocks, use of nontoxic biodegradable solvents for purification, mild reaction conditions and simplicity of the reaction.

TABLE 2.5
Green metrics results for each of the FAAms

Product	%AE	sEF	cEF	EcoScale
C+4	91.70	1.22	44.18	69.00
C+8	92.80	1.06	36.20	76.50
C+12	93.60	1.06	44.82	72.00
C+16	94.30	0.67	41.30	80.00
S+4	91.70	1.00	40.03	72.50
S+8	92.80	1.17	38.26	74.50
S+12	93.60	1.03	43.86	73.00
S+16	94.30	0.61	39.43	81.50
P+4	91.70	0.95	38.42	74.00
P+8	92.80	1.12	37.27	75.50
P+12	93.60	1.16	46.49	71.00
P+16	94.30	0.59	38.51	82.50

3. MICROENCAPSULATED PHASE CHANGE MATERIALS (μPCM)

3.1 Background

Since conventional asphalt pavement is black, it has a strong heat-absorbing capacity (Chen et al., 2011) and can reach temperatures as high as 70°C during peak sunlight conditions (Chen et al., 2012). The air temperature in urban cities is higher when compared to rural areas because of the high volumetric heat capacity and reduced evapotranspiration of concrete and asphalt, the two main materials used in buildings, roads, and parking lots. This phenomenon is known as the urban heat island (UHI) effect and has many environmental and health issues (He et al., 2013). Areas that suffer from UHI have higher water and energy consumption and contribute to the acceleration of smog production (Guan et al., 2011; Gui et al., 2007). Furthermore, when asphalt reaches high temperatures, the binder's viscosity and adhesion properties decrease. This results in a lower asphalt mixture stiffness that can lead to large permanent deformation under repeated loading, a distress commonly manifested as asphalt rutting (Chen et al., 2011; Sun, 2016).

Several methods to lower the temperature of asphalt during the summer have been considered, such as spraying water on the pavement and using porous pavement, however, they have not been effective or practical (Cao et al., 2011). A novel and different approach that could be used to prevent asphalt pavements from reaching such high temperatures is the use of PCMs. PCMs are substances that absorb significant amounts of energy from their surroundings when they melt, while remaining at a constant or approximately constant temperature (Liston et al., 2016). This energy that is absorbed is known as latent heat of fusion and it is transferred back to the surroundings when the PCM goes back to the solid state (Fleischer, 2015). This particular property of PCMs make them suitable materials to be incorporated in asphalt to help regulate its temperature and decrease the UHI effect and avoid/delay rutting.

As it was mentioned before, PCMs can be used in many applications related to thermal energy storage and management such as in textiles (Mondal, 2008), buildings (Kalnæs & Jelle, 2015), and solar energy storage systems (Kenisarin & Mahkamov, 2007). However, since these materials need to transition from the solid to the liquid state to fulfill their function, they must be contained to avoid their leakage during the liquid phase (Fleischer, 2015). The use of PCMs in asphalt pavements poses a series of challenges that are not encountered in other applications. Perhaps the most difficult one is to find a containment system that can keep the PCM from leaking at the high temperatures and under typical mechanical loadings of asphalt mixture production. Partially successful results have been obtained in studies where the PCMs were shape stabilized using porous aggregates as carriers (Manning et al., 2015). However, it was found that PCMs in these systems are prone to evaporate at asphalt mixture processing temperatures. This issue has been addressed by coating the carrier aggregates using polymeric resins (Kheradmand et al., 2015). Nonetheless, this decreases the overall PCM content in the aggregate along with their thermal conductivity.

Another alternative for PCM containment is their microencapsulation in core-shell structures made of polymeric materials. This method of PCM microcapsules is popular in building walls, however, only a few investigations have been conducted to incorporate them in asphalt pavements. This is likely because most polymeric materials do not perform well at high temperatures, making these capsules incompatible with asphalt mixture production conditions. The work reported here studies the feasibility of adding PCM microcapsules with high thermal stability and robust walls to asphalt pavements to decrease their peak temperatures, potentially alleviating issues such as UHI effect and pavement rutting.

3.2 Methods

3.2.1 Characterization of PCM Microcapsules

Commercially available PCM microcapsules (μPCM-43) were purchased from Microtek labs due to their high thermal stability (less than 1% leakage when heated up to 250°C (482°F)) and their robust capsule walls (Microtek Laboratories, n.d.). These features should help the capsules withstand asphalt processing conditions and allow them to perform their thermal management role. These capsules are expected to exhibit high latent heat of fusion (220–230 J/g) and small sizes which translate into high surface area and will likely improve heat transfer, helping counteract the low thermal conductivity typical of these materials (Farid et al., 2004). The experimental transition temperatures and latent heats of the microencapsulated PCMs were corroborated using a Q2000 DSC analyzer (Q2000 DSC TA Instruments). Experiments were conducted in a nitrogen atmosphere with cooling and heating rates of 10°C/min. TGA (Q50, TA Instruments) was also conducted to study the thermal stability of the capsules at asphalt mixture production temperatures. Samples were ramped at 15°C/min from room temperature to 600°C. Isothermal experiments at 165°C (329°F) for 3 hours were completed as well. Images of the capsules were taken using a scanning electron microscope (Phenom, FEI Company) for which the samples were previously mounted and coated with a thin layer of platinum (~10 nm) using a sputter coater (K550X Emitech) for 30 s.

3.2.2 Ball Milling Experiments

In order to use PCM microcapsules in asphalt pavements they not only need to be thermally stable but must be able to withstand compression and shear stresses typical of the mixing and compacting of asphalt

mixtures. To assess the mechanical performance of the microcapsules, ball milling experiments were also conducted followed by a visual inspection using an optical microscope. For this, 0.7 g of microcapsules and 14 g of tungsten carbide balls (3 mm in diameter) were added to a 25 ml glass vial and then placed inside an oven at 145°C (293°F) for 2 hours. Next, the vial was removed from the oven, capped, and immediately milled using a wheel mixer (30 rpm) for 20 minutes at room temperature.

3.3 Deliverables

3.3.1 Phase Change Material Load Analysis

The amount of PCM required to change the temperature of asphalt pavement by 1°C was roughly estimated using Equation 3.1 (Bureau of Naval Personnel, 1966).

$$Q = m \cdot C \cdot \Delta T \qquad \text{(Equation 3.1)}$$

where Q is the amount of heat (in J) required to produce a temperature difference or ΔT (in °C), m is the mass of the sample undergoing the temperature change (in Kg), and C is the specific heat capacity of the sample (in J/Kg•°C). The amount of heat required to decrease the temperature by 1°C of a 2-in.-thick asphalt slab with a length and width of 1 m and a mass of 115.6 Kg was estimated to be –110.88 KJ (for an asphalt sample with ρ = 2,276 Kg/m^3 and C = 959 J/Kg•°C (Vo et al., 2015)). The minimum amount of PCM needed to achieve this temperature change would be 0.55 Kg (for a PCM with a latent heat of 200 J/g), assuming there are no heat losses in the system and no heat is being transferred from or to the asphalt pavement and its surroundings. The necessary 0.55 Kg of PCM would be the equivalent to 0.5% of the total slab mass. It must be noted that these calculations are not expected to be representative of the actual amount of PCM needed to induce the mentioned temperature change since several variables such as heat losses in the system, and the thermal conductivity and diffusivity of the materials were not considered. This theoretical value was used to determine the order of magnitude in which the PCM must be added. To ensure that the thermal regulation action of the PCM would be seen in the thermal cycling tests, the PCM microcapsules were added between 2% and 8% of total mixture mass to the asphalt mixtures prepared in Chapters 4 and 5.

3.3.2 μPCM-43 Visual Inspection

As seen in Figure 3.1, the μPCM-43 presented spherical shapes and a wide size distribution (2–25 μm). Interestingly, most capsules have dents in them. It must be noted that this micrograph was taken at room temperature, hence, the PCM cores are expected to be in the solid state. It is highly possible that the dents were produced by volumetric changes experienced by the core during their phase change from liquid to solid, which for paraffins can be around 10% (Cabeza et al., 2020). However, even when most capsules look dented, they do not appear to have cracks, indicating that the shell is sufficiently strong and flexible to sustain these volumetric changes.

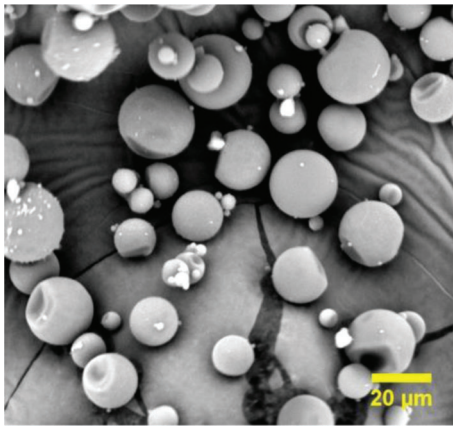

Figure 3.1 SEM micrograph of the PCM microcapsules, μPCM-43.

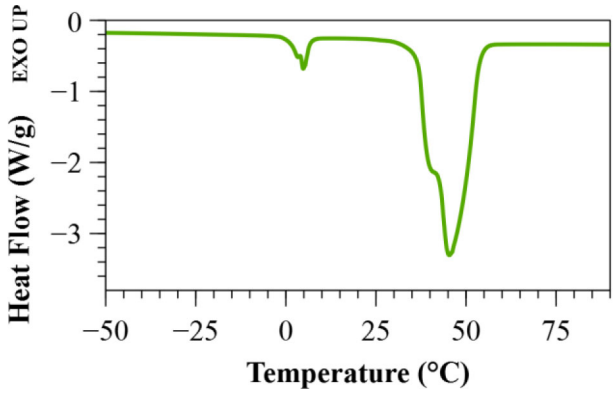

Figure 3.2 DSC thermogram of PCM microcapsules.

As seen in the thermogram presented in Figure 3.2, the microcapsules exhibited two separate events for both melting and crystallization transitions; the first and minor melting event takes place around 5°C with a latent heat of approximately 9.6 J/g. The second and main melting event has an onset around 36.5°C and reaches its peak at ~45°C. It is possible that the difference between the experimental melting point and that reported by the manufacturer (43°C) was a consequence of the fast-heating rate (10°C/min) used during the experiment. The heat of fusion was ~200 J/g which is 20–30 J/g below the manufacturers' specification. However, these differences in melting point and latent heat are not significant for the project and should not affect the PCM's ability to regulate the asphalt mixture's temperature. Figure 3.2 also shows that each transition event shows two humps or overlapping peaks. It is possible that the PCM contained in this capsule is based

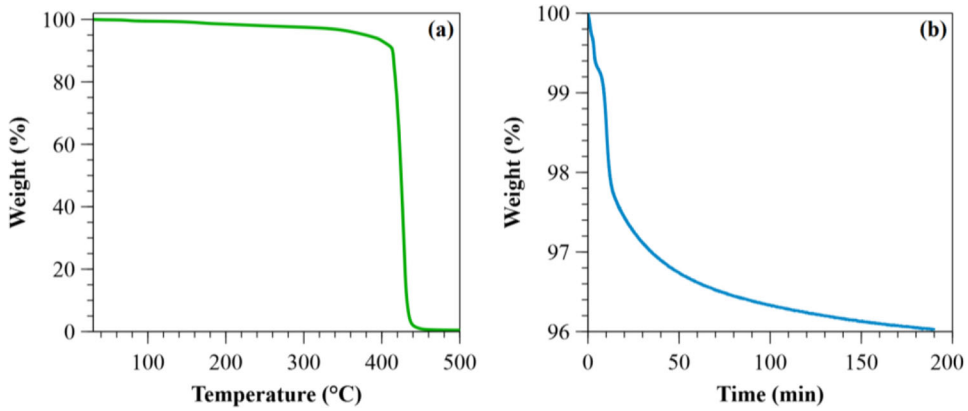

Figure 3.3 TGA thermograms of PCM microcapsules (a) temperature ramp from room temperature to 400°C (15°C/min), and (b) isothermal at 165°C.

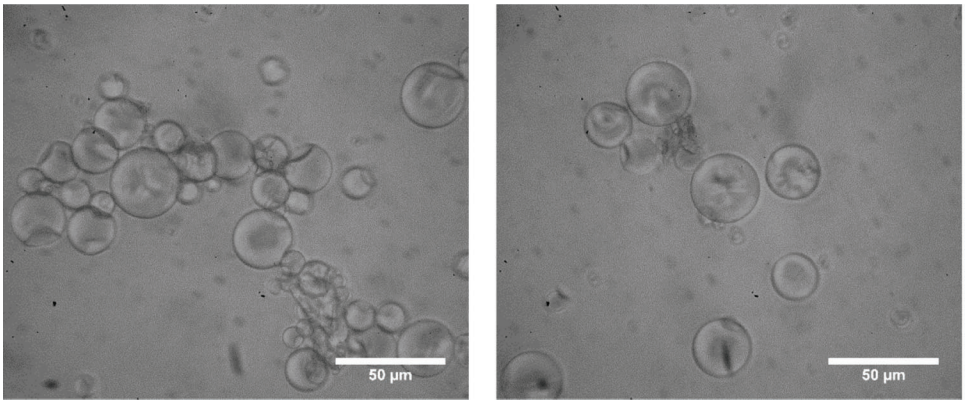

Figure 3.4 Optical micrographs of microcapsules after the ball milling experiment.

on a blend of two or more paraffins which were mixed to tune the melting temperature of the resulting substance (Farid et al., 2004; Kousksou et al., 2010).

The thermal stability of the capsules was studied by performing two different experiments. In the first one, the capsules' temperature was increased at a constant rate (15°C/min) from room temperature to 500°C. Results presented in Figure 3.3(a) show that the capsules degrade at approximately 410°C (770°F) when they lose most of their mass (~90 wt.%) due to PCM evaporation. To simulate asphalt production conditions, the second experiment consisted of increasing the capsules' temperature to 165°C (329°F) and keeping it constant for 3 hours. The thermogram in Figure 3.3(b) indicates that the sample only lost 4% of its weight during this test. This weight loss probably corresponds to the PCM evaporation of inherently imperfect capsules in the production batch. Considering how small these weight losses are, results confirm that the microcapsules are stable at asphalt production temperatures (about 135°C–162°C or 275°C–325°F).

3.3.3 Ball Milling Experiment Results

Micrographs of the capsules taken after the ball milling experiment are presented in Figure 3.4. Unfortunately, it was not possible to precisely determine the ratio of broken capsules for several reasons—first, agglomerates formed during testing and could not be entirely broken apart to assess the capsules' individual integrity. Second, the micrographs only allow imaging of a partial section of the capsules, hence even when they may look whole from the top they could be broken on the bottom. However, to obtain a rough estimate, all the capsules that exhibited a circular contour after the test (despite being dented) were considered whole, while those with irregular shapes and flat appearance were counted as broken (signaled by black arrows in Figure 3.4). Based on this analysis roughly 10% of the capsules broke, or in other words, close to 90% of the capsules survived the ball milling experiment. This survival rate is high considering that the capsules are made of polymers (unknown composition due to proprietary rights) which usually soften and underperform at high temperatures. Nonetheless, even if only 10% of the capsules break this could translate in a significant amount of PCM being released and could likely have a detrimental effect on the mechanical properties of the asphalt pavement. The direct interaction of PCM with asphalt can decrease the penetration and decrease the softening point and stiffness of the binder (Kakar et al., 2020).

4. RHEOLOGICAL AND THERMAL PERFORMANCE OF μPCM MODIFIED ASPHALT MATERIALS

4.1 Background

It is hypothesized that comprehensive thermomechanical testing can characterize and optimize μPCM modified asphalt binders and mixtures. However, research to-date has not yet determined prevalent tests and parameters that can be used to explain the performance of μPCM modified asphalt binders and mixtures, develop standard specifications, and link binder and mixture behavior. As a step toward this goal, this chapter's overall research objective is to identify testing techniques that characterize the thermomechanical performance of μPCM modified asphalt binders and mixtures within the linear viscoelastic range. This portion of the study introduces a new approach to identify the μPCM effect in asphalt binders using rheological measurements. Additionally, the findings of this section of the study corroborate experimental and numerical investigations showing that a reduction in pavement surface temperatures between 2°C and 9°C can be obtained with μPCM modified asphalt materials, as compared to non-μPCM modified asphalt materials (Jin et al., 2017; Refaa et al., 2018).

4.2 Methods

4.2.1 Asphalt Binder Testing

For asphalt binder testing, a control binder was mixed with the μPCM-43 at 160°C (320°F) using a mechanical agitator for 5 minutes. Although the μPCM capsules exhibit good temperature stability, the mixing process took place just before specimen preparation. A PG 64-22 asphalt binder was used for this portion of the study. In this chapter, the rheological properties of μPCM-43 modified asphalt binders were characterized using recently explored testing techniques. The Dynamic Shear Rheometer (DSR) test protocol employed is based on the methods reported by Kakar et al. (2019a) and Kakar et al. (2019b). The thermal effect of μPCM-43 on the modified asphalt binder's rheological response was determined by performing temperature sweep tests. The dynamic shear properties were measured using the parallel plate configuration of 2-mm-thick specimens with a 8-mm diameter. Temperature ramps from 60°C to 20°C (and vice versa) were conducted while applying an oscillatory shear strain with constant strain amplitude (1.0%) and frequency (10 rad/s). These testing inputs were selected to keep the rheological measurements within the linear viscoelastic range and equipment torque limits.

The control PG 64-22 binder was modified at six different levels, 0%, 5%, 10%, 20%, 30%, and 40% by total binder mass. In addition, the rheological testing was conducted at five different temperature ramps between 60°C and 20°C, namely 3, 6, 9, 12, and 15°C/hr. For each binder-μPCM combination, a single specimen was examined. After loading the specimen in the DSR, the material was initially conditioned for 20 minutes at 60°C. Then, the rheological testing equipment was configured to run a cooling-heating cycle for each temperature rate. The DSR Peltier system decreased the temperature from 60°C to 20°C within a specific time duration and increased the temperature from 20°C to 60°C within the same time span. The temperature ramps were conducted successively from slowest to fastest, without interruptions. The set of temperature ramps used is comparable to the temperature change rates experienced by in-service asphalt pavements (Yavuzturk et al., 2005). The viscoelastic properties were measured at 30-second intervals, meaning that every 30 s, the DSR decreased a temperature step and reported the average results of the rheological measurements continuously taken within the time step. Rheological measurements were complemented with DSC tests.

4.2.2 Asphalt Mixture Thermal Cycling

The thermal response of μPCM modified asphalt mixtures was also investigated. First, four asphalt mixtures gathered from three paving projects were modified with PCM microcapsules at three different levels, 0%, 4%, and 8% by total mixture mass. Figure 4.1 shows the characteristics of these mixtures. Mixture A was gathered from a paving project near Crawfordsville, IN, Mixture B from a pavement reconstruction section in Indianapolis, IN, and Mixtures C and D from a pavement overlay project near Fort Wayne, IN. Mixtures C and D have comparable aggregate blends, with the main difference being that Mixture C includes steel slag aggregate (Haddock et al., 2020).

The plant-produced paving materials were heated in the laboratory at 135°C (275°F) for 2 hours and then manually mixed with μPCM-43 until all the particles exhibited a dark appearance (about 5 minutes), as shown in Figure 4.1a. The μPCM-43 modified asphalt material was again placed in the oven for approximately 20 minutes to get back to the 135°C (275°F) established temperature for compaction. About 2,700 g of mixture were compacted using the Superpave Gyratory Compactor (SGC) to a specific height of 63.5-mm (2.5 in.), or until a total of 50 SGC gyrations were reached. Little information is available in the literature regarding the compaction and fabrication of μPCM modified asphalt mixture specimens. Thus, a 63.5-mm (2.5 in.) height was specified to ensure that 50-mm (2-in.) tall specimens could be fabricated for thermal cycling experiments. However, during compaction, it was observed that all the specimens were compacted until the number of gyrations criterion was achieved, except the control specimen for Mixture C. The specimens modified with μPCM at 0%, 4%, and 8% by total mixture mass were compacted to an average height of 65.5 mm, 68.6 mm, and 76.2 mm, respectively.

Following compaction, the SGC pills were cut using a saw to fabricate 50-mm (2-in.) tall specimens.

Figure 4.1 (a) Mixing process of μPCM-43 and asphalt mixture and (b) specimens prepared for thermal cycling, Mixture B.

Subsequently, three type-T thermocouples were placed on each specimen, one at the top surface (non-insulated circular face), one 25 mm (1 in.) from the top surface (mid-specimen), and one at the bottom surface. The mid-specimen temperature sensor was mounted at the center by drilling a hole to fit the thermocouple. Thermally conductive adhesive tape was applied to secure the thermocouples at the bottom and top surfaces. The specimens' bottom surface and outside diameter were then insulated using a 50-mm (2-in.) insulating board to produce a one-dimensional heat flow during thermal cycling testing (see Figure 4.1b). To further minimize heat loss, the gap between the specimen and insulating board, plus the incisions made in the board to place the thermocouples, were filled with an insulating foam sealant. After insulating and instrumenting the specimens, they were placed in an environmental chamber and exposed to a heating-cooling temperature cycle. For the purpose of capturing the μPCM effect at about 43°C, the specimens were subjected to liquification and solidification transitions from 20°C to 60°C and from 60°C to 20°C, respectively.

Volumetric analysis was performed on the SGC pills before dimensioning the specimens to a 50 mm (2 in.) height. Despite the changes in SGC specimen mass and reduction in mixture design compaction temperature, from the 150°C (300°F) allowed by the Indiana Department of Transportation (INDOT) specifications, to the 135°C (275°F) used for this study, the air voids contents of the control mixtures' specimens fell within the permissible range. However, the air voids contents of the compacted μPCM-43 asphalt mixture specimens were out of the specification limits, between 3.6% and 6.4%. The air voids contents of the μPCM-43 modified asphalt mixtures' specimens were significantly below the lower specification limit. Not surprisingly, as more μPCM-43 capsules were included, the air void content departed even more from specifications. These volumetric results strengthen the argument that for the inclusion of μPCM-43 in asphalt mixtures, a portion of fine aggregate and mineral filler from the original mixture design should be replaced with μPCM-43 to satisfy the volumetric requirements (Bueno et al., 2019; Refaa et al., 2018). Some μPCM-43 modified specimens showed an air voids content even lower than 1%. To improve the feasibility of this technology, an appropriate mixture design procedure will need to be developed.

4.3 Deliverables

4.3.1 Complex Shear Modulus Change Rate

Studies into the viscoelastic behavior of asphalt binders have received increased interest from various researchers since the early 1990s, following the Strategic Highway Research Program (SHRP) (Anderson et al., 1994; Yusoff et al., 2011). The SHRP research effort reported that over most of the range of interest in asphalt binder applications, the rate of change of Complex Shear Modulus (G*) with respect to temperature ranges from 15% to 25% per degree Celsius (Anderson et al., 1994), which means that asphalt binders should exhibit a relatively constant G* Change Rate when subjected to a continuous temperature gradient. Such a concept has not been thoroughly investigated over the years, in significant part because of equipment limitations. Many of the commercial rheological testing devices available in the early 1990s were designed primarily for use with polymers, foodstuffs such as cheese, and other materials, many of which exhibit low temperature dependency in comparison to asphalt binder (Anderson et al., 1994). In such a situation, most rheological testing devices provided just enough temperature control accuracy for maintaining suitable repeatability of test data. Consequently, as per

specifications, asphalt binder tests are typically performed under steady-state temperature conditions. However, today, rheological testing devices can perform temperature fluctuations and ramps with a great deal of accuracy. Some rheological testing devices can even guarantee a homogeneous convection temperature distribution and thus, accurate and stable temperature control for various testing protocols.

Figure 4.2a confirms that an asphalt binder subjected to a constant temperature increase (from 20°C to 60°C) will show a relatively constant G* Change Rate. This calculation will vary depending on the temperature ramp applied and the interval at which rheological measurements are taken. For this study, the measurements were taken at 30-second intervals. This time step is used to calculate the G* Change Rate, as shown in Equation 4.1.

$$G^* \, Change \; Rate = \frac{G_i^*}{G_{i-1}^*} \qquad \text{(Equation 4.1)}$$

where G_i^* is the complex shear modulus at a given temperature and G_{i-1}^* is the complex shear modulus obtained at the previous time step for the predetermined temperature change rate during the solidification or liquification cycle phase.

Data from several studies have demonstrated that the temperature can be shifted or reduced by incorporating

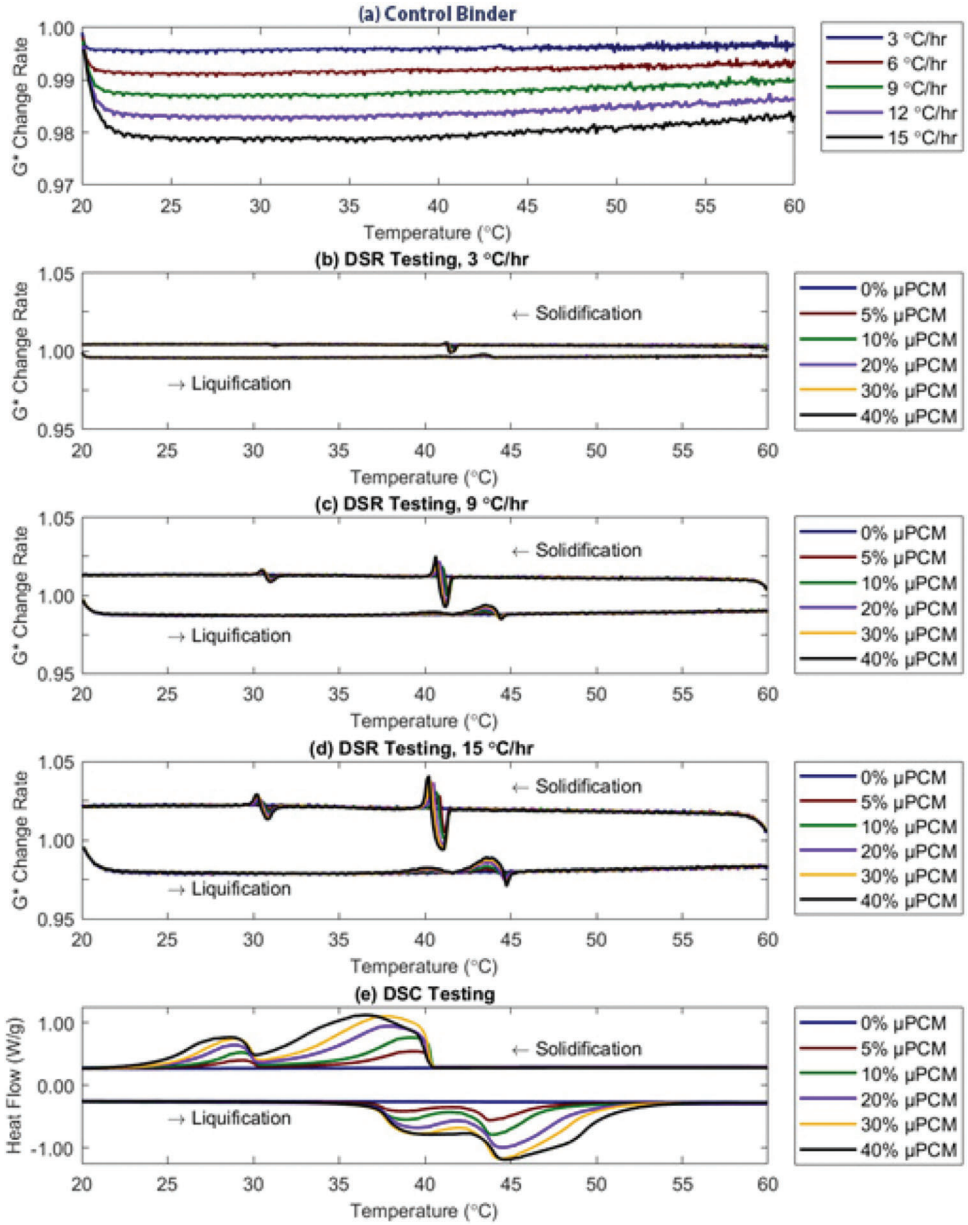

Figure 4.2 Asphalt binder experiments using dynamic shear rheometer and differential scanning calorimeter.

μPCM into asphalt binders (Kakar et al., 2019a; Kakar et al., 2019b; Refaa et al., 2018; Wei et al., 2019). Although previous studies have encouraged the use of DSR measurements, a method to fully understand the μPCM effect in asphalt binders using rheological data was not identified. For example, Kakar et al. (2019b) modified control asphalt binders with μPCM having a phase transition temperature close to 6°C, at three different levels, 0%, 1%, and 3% by total binder mass. In their research study, the rheological measurements were taken by performing temperature ramps between 20°C and -10°C, using a cooling-heating rate of about 26°C/hr. The constant strain amplitude and frequency applied to run the tests were 0.1% and 6.3 rad/s, respectively. The rheological measuring system had a diameter of 8 mm and specimen thickness of 2 mm. To interpret the results, master curves, complex shear modulus versus temperature, and phase angle versus temperature plots were generated. After analyzing the data, Kakar et al. (2019b) suggested that during cooling ramps, no thermal effect due to μPCM incorporation is noticed on the rheological response of modified asphalt binders, and concluded that perhaps at higher μPCM concentrations, the effect could be detectable. The work presented herein differs from previous research regarding the idea that a μPCM effect cannot be captured by performing rheological measurements. If the data is normalized utilizing the G* Change Rate, the μPCM effect is noticeable during solidification and liquification transitions, at low and relatively high μPCM dosages, and temperature fluctuations comparable to those experienced by asphalt pavements in the field.

Figure 4.2 shows that the rate of change concept can help quantify the μPCM effect in asphalt materials. This rheological data analysis is in good agreement with the results obtained from DSC measurements, as can be inferred from Figure 4.2e. The evidence is murky because DSC measurements were performed at a cooling-heating rate of 600°C/hr (or 10°C/min), which is a typical testing parameter for this thermal procedure. This cooling-heating rate is inconceivable for the rheological analysis of asphalt binders. Although DSC measurements were performed at a significantly higher cooling-heating rate, the μPCM effect peaks observed are connected to the rheological results obtained at cooling and heating rates between 3 and 15°C/hr. When the μPCM-43 releases heat (solidification phase), a reduction is observed in the G* Change Rate, primarily due to a thermal lag in the asphalt binder specimen. The specimen is no longer transitioning at a constant temperature rate because of the μPCM-43. In contrast, when the μPCM-43 absorbs heat (liquification phase) from the system, an increase is noticed in the G* Change Rate, meaning the DSR must apply a higher torque (or activation energy) to generate the predetermined strain amplitude of 1.0% in the asphalt binder specimen. In both phases, a countereffect is observed in the rheological measurement after the μPCM-43 effect is completed, as compared to

TABLE 4.1
Asphalt mixtures used for thermal cycling assessment

Mixture Name	Mixture A	Mixture B	Mixture C	Mixture D
Mixture Description	Surface Mainline	Base Mainline	Surface Mainline	Surface Shoulder
Mixture Designation (mm)	9.5	19.0	9.5	9.5
Binder Type	PG 70-22	PG 64-22	PG 76-22	PG 64-22
Aggregate Material	9.5-mm Dolomite 4.75-mm Dolomite 2.36-mm Dolomite Sand 9.5-mm RAP Mineral Filler	19.0-mm Stone 9.5-mm Stone 4.75-mm Stone 2.36-mm Stone Sand 12.5-mm RAP 9.5-mm RAP Mineral Filler	9.5-mm Limestone 4.75-mm Limestone 9.5-mm Steel Slag 2.36-mm Manufactured Sand 9.5-mm RAP Mineral Filler	9.5-mm Limestone 4.75-mm Limestone 2.36-mm Natural Sand 2.36-mm Manufactured Sand 9.5-mm RAP Mineral Filler
Air Voids Content (%)	5.0	5.0	5.0	5.0
Voids in the Mineral Aggregate (%)	16.6	14.7	16.9	17.1
Voids Filled with Asphalt (%)	69.9	66.0	70.4	70.8
Asphalt Binder Content (%)	6.1	5.4	5.8	6.5
Effective Binder Content (%)	4.9	4.2	4.9	5.3
Virgin Binder (%)	4.6	4.6	4.7	5.6
Binder Replacement (%)	24.3	15.4	19.7	13.8
Dust-to-Binder Ratio	1.0	1.2	0.9	0.8
Number of Design Gyrations	50	50	50	50
SGC Pill Mass (g)	4,825	4,700	5,140	4,860

DSC results. A possible explanation for this might be that the binder experiences an accelerated temperature transition. There might be a significant temperature gradient between the DSR plates and μPCM-43 modified binder due to the thermal lag, causing a sudden temperature shift in the specimen. Additionally, in DSR testing the asphalt binder is susceptible to heat losses as opposed to DSC testing, where the specimen is enclosed in a thermal chamber. More research is necessary to understand the cause of this countereffect and its potential ramifications.

The rheological results are also consistent with the present evidence suggesting that under different cooling and heating rates, the intensity of the latent heat peak is augmented because thermal gradients are built up in the PCM. A study on the phase change process and latent heat of PCM impregnated lightweight aggregate (LWA) concluded that DSC tests with higher cooling and heating rates intensify the verticality of the curve at the peak temperature (Kheradmand et al., 2015). Likewise, the rheological results of this study demonstrate that as the cooling-heating rate increases, the peak of the G* Change Rate is intensified, as shown in Figures 4.2b–d. It should be noted that regardless of the cooling-heating rate in DSC testing, the amount of latent heat absorbed and released by the μPCM-43 is constant. This fundamental concept can be demonstrated by calculating the integral under the DSC peak above the baseline (Kheradmand et al., 2015). The analogous DSR and DSC plots suggest that a similar analysis might be applicable for the rheological results. Although the rheological findings should be treated with a degree of caution, the results are interesting because they identify an approach for capturing the μPCM effect in asphalt binders. This analysis warrants further investigations to correlate the G* Change Rate to the latent heat capacity of the μPCM-43 modified asphalt binders and their overall mechanical performance. Table 4.2 reports the latent heat characteristics of μPCM-43 modified asphalt binders according to the DSC measurements.

4.3.2 Thermal Cycling of Asphalt Mixtures

Figure 4.3 shows the thermal response of asphalt specimens with and without μPCM-43. The control asphalt mixture is a 9.5-mm plant-produced mixture gathered in-situ through plate sampling on the road, namely Mixture A. The specimens were exposed to a temperature cycle between 20°C and 60°C to capture the μPCM effect at about 43°C. When the μPCM particles liquify, the μPCM-43 product delays the modified asphalt specimens from reaching a threshold temperature of 45°C and creates a thermal lag in the specimens. As a result, the temperature of the μPCM modified asphalt specimens dwells at about 43°C for a longer time than if the μPCM was not present. Likewise, during solidification, the μPCM effect provides additional relaxation time to the asphalt specimen during the temperature transition from 60°C to 20°C, at approximately 43°C. A closer examination reveals that a second thermal lag is experienced at about 30°C when the μPCM-43 is cooling. This observation is more evident for the specimen modified with 8% μPCM-43 by total mixture mass. Overall, the thermal responses of the μPCM-43 modified asphalt specimens mimics the rheological analysis found for the asphalt binders, as presented in the previous section. As the μPCM-43 solidifies, two sharp peaks are detectable for the G* Change Rate, at about 43°C and 30°C. Conversely, when the μPCM-43 is transitioning to a liquid, the DSR, DSC, and thermal cycling measurements agree that the μPCM effect occurs more uniformly between 35°C and 45°C. Similar observations can be made for the other three asphalt mixtures tested, Mixtures B, C, and D (see Appendix B).

Table 4.3 reports the differences in temperature obtained at different depths from the top surface for the specimens with μPCM-43 relative to the control specimens. The liquification (from 20°C to 60°C) and solidification (from 60°C to 20°C) μPCM-43 transitions demonstrate disparities in the absolute temperature differences observed. During PCM solidification, the temperature differences are consistently lower for all mixture types. Thus, the μPCM-43 appears to be more beneficial when liquifying, meaning that the μPCM-43 does a better job delaying the appearance of temperatures higher than 43°C in comparison to hindering temperatures lower than 43°C. This outcome is contingent on the type of μPCM and ambient temperature profile, along with other factors. Still, at first glance, the μPCM-43 effect seems promising in delaying temperatures above 45°C. The μPCM impact is more meaningful as the depth from the top surface increases. Another important observation of this study is that the thermal cycling tests included mixtures composed of a wide variety of raw materials. The A, B,

TABLE 4.2
Differential scanning calorimeter test results for μPCM-43 modified asphalt binders

μPCM-43 Content by Binder Mass (%)	Solidification Phase		Liquification Phase	
	Temperature Range (°C)	Latent Heat (J/g)	Temperature Range (°C)	Latent Heat (J/g)
5	29.3–39.5	8.3	38.5–43.8	8.8
10	29.3–39.1	16.4	38.8–44.0	16.8
20	28.9–37.9	31.1	39.3–44.5	31.6
30	28.9–37.7	42.7	39.4–42.4	42.8
40	28.6–36.7	50.7	39.5–44.5	50.7

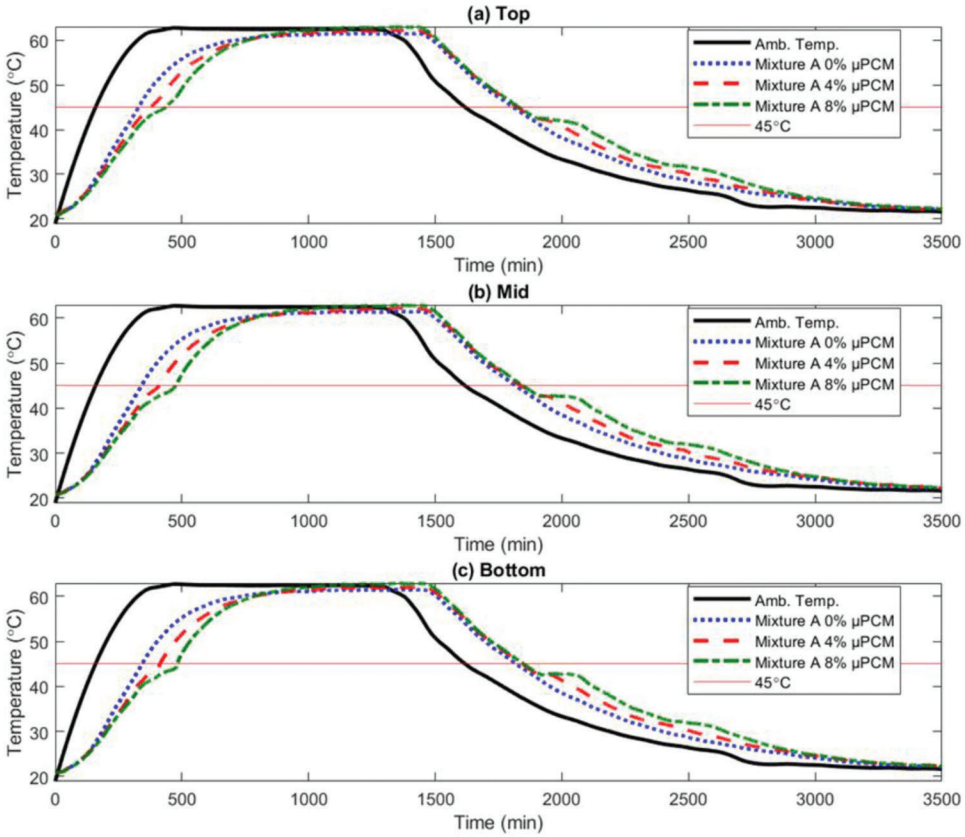

Figure 4.3 Mixture A thermal response of asphalt specimens with and without μPCM-43 at different depths from top surface.

TABLE 4.3
Absolute maximum temperature difference between control and μPCM-43 modified specimens

Control Mixture	μPCM-43 Content by Total Mixture Mass (%)	Phase Transition	Absolute Maximum Temperature Difference (°C)		
			Depth from Top Surface (mm)		
			0 (Top Surface)	25 (Mid-Specimen)	50 (Bottom Surface)
Mixture A	4	Liquification	4.64	5.68	6.16
		Solidification	2.61	2.81	2.92
	8	Liquification	7.93	9.48	10.13
		Solidification	4.56	5.22	5.43
Mixture B	4	Liquification	4.70	5.27	6.25
		Solidification	2.70	3.04	3.32
	8	Liquification	6.10	8.46	9.30
		Solidification	3.53	4.66	4.99
Mixture C	4	Liquification	4.72	5.62	6.29
		Solidification	2.47	2.85	3.19
	8	Liquification	7.53	9.06	10.32
		Solidification	4.10	4.74	5.46
Mixture D	4	Liquification	3.74	5.65	6.34
		Solidification	1.91	2.89	3.15
	8	Liquification	7.23	8.83	9.64
		Solidification	3.75	4.39	4.64

C, and D Mixtures were gathered as part of a research project focused on implementing asphalt mixture design changes in Indiana (Haddock et al., 2020). As a result, the mixtures used in the experiments come from various areas of the state. Consequently, the thermal cycling results suggest the μPCM effect is applicable for a broad array of asphalt mixture materials.

5. MECHANICAL PERFORMANCE OF μPCM MODIFIED ASPHALT MATERIALS

5.1 Background

As previously explained, the past decade has seen the rapid development of μPCM for diverse engineering applications (Jamekhorshid et al., 2014), aiding the incorporation of this thermoregulating agent in asphalt materials. As a result, more recent attention has focused on conducting mechanical performance tests for μPCM modified asphalt binders and asphalt mixtures. The rheological behavior of μPCM modified asphalt binders has been studied using conventional and unconventional testing protocols (Kakar et al., 2019a; 2019b; Wei et al., 2019). In contrast, μPCM modified asphalt mixtures' mechanical performance has been mainly examined by conducting standard test protocols (Bueno et al., 2019), while the role of μPCM on the engineering behavior of compacted asphalt mixture specimens remains largely unexamined. Further studies are required to fully quantify the μPCM effect on the performance of asphalt pavements. Several questions regarding the mechanical characterization of μPCM modified asphalt materials remain to be addressed. For example, the thermomechanical response of μPCM modified asphalt materials when the core PCM is in solid or liquid phase. There is a lack of standard methods for testing the PCM in asphalt materials and assessing the suitability of a given μPCM formulation to a specific asphalt pavement environment or target asphalt mixture distress. Investigations are needed to develop procedures that allow comparison and evaluation for μPCM modification in asphalt pavements. Given such information, this chapter seeks to obtain data that will help to address these research gaps. The redesign of an asphalt mixture with μPCM is demonstrated, and the mechanical performance implications of incorporating a significant portion of μPCM in the binder and mixture are discussed.

5.2 Methods

5.2.1 Redesign of Asphalt Mixture

Table 5.1 illustrates how a reference mixture was redesigned to incorporate a significant portion of μPCM-43, at two different levels (about 2% and 4% by total mixture mass). The reference mixture had the same aggregate blend and volumetric properties of mixture A (see Table 4.1), but it was prepared using a PG 64-22 asphalt binder. All the material passing the 0.300- and 0.600-mm sieves was substituted with microcapsules for the 2%- and 4%-μPCM-43 mixtures, respectively. Considering that the capsules have a specific gravity of about 0.900, the replacement was estimated by volume and not by mass. Therefore, all the substituted fine aggregate and mineral filler material was assumed to have a specific gravity of 2.800.

First, the aggregate was batched as typically done for specimen fabrication. After batching, the aggregate was sieved to determine the mass of the material to be substituted. Then, the approximate volume of the material passing the critical sieve for each redesigned mixture was calculated by dividing its total mass by 2.800. The estimated volume was multiplied by 0.900 to obtain the mass required to produce a similar volume replacement of μPCM-43. The mass of the virgin PG

TABLE 5.1
Batching for μPCM-43 redesigned asphalt mixtures

		Component Mass (g)		
	Component	**Reference Mixture**	**2% μPCM-43 Mixture**	**4% μPCM-43 Mixture**
Retained Sieve Size (mm)	12.5	0.0	0.0	0.0
	9.5	348.4	348.4	348.4
	4.75	2,533.9	2,533.9	2,533.9
	2.36	1,796.3	1,796.3	1,796.3
	1.18	1,036.6	1,036.6	1,036.6
	0.600	587.9	587.9	587.9
	0.300	353.4	353.4	0.0
	0.150	179.1	0.0	0.0
	0.075	66.9	0.0	0.0
	Pan	172.1	0.0	0.0
	μPCM-43	0.0	134.4	248.0
	PG 64-22 Asphalt Binder	325.4	325.4	325.4
	Total Mass	7,400.0	6,981.9	6,876.5
Proportion of μPCM-43 by Total Mixture Mass (%)		0.0	1.9	3.6
μPCM-43 to Virgin Binder Ratio (%)		0.0	41.3	76.2
Maximum Specific Gravity		2.544	2.424	2.341

Note: Red text indicates retained material at the sieves in the reference mixture were substituted with μPCM-43 for redesigned mixtures.

64-22 asphalt binder was kept the same for the μPCM-43 redesigned mixtures. The retained material above the critical sieves and virgin binder were heated at 135°C (275°F) for 2 hours and then mixed in the laboratory. Following mixing, the asphalt mixtures were short-term conditioned for mixture mechanical property testing at 135°C (275°F), in accordance with AASHTO R 30-02. After conditioning, the μPCM-43 particles were added and manually mixed to the laboratory-prepared mixture until all the μPCM-43 particles looked coated with asphalt binder (about 5 minutes). The μPCM-43 modified asphalt mixtures were again placed in the oven for approximately 20 minutes to regain the 135°C (275°F) required temperature for compaction. The modification is reported by the masses of raw material needed to prepare SGC specimens that were 180 mm (7 in.) in height (see Figure 5.1a) from which specimens with air voids content of $5.0 \pm 0.5\%$ could be extracted for mechanical testing. The same batching and mixing procedures were performed to prepare the required amount of material to determine each mixture's theoretical maximum specific gravity (G_{mm}), according to AASHTO T 209-19.

A wide variety of PCM dosages have been investigated in experimental and numerical studies. The proportions of μPCM-43 by total mixture mass evaluated in this study are in good agreement with recent investigations and comparable to those reported in the literature (Bueno et al., 2019; Jin et al., 2017; Kakar et al., 2019a; 2019b; Ma et al., 2019; Wei et al., 2019). Perhaps the most interesting aspect of this study is the variation in aggregate components to allow for μPCM incorporation. Few studies have attempted to entirely redesign an asphalt mixture using μPCM. Instead, most investigations have added the μPCM directly to an existing asphalt mixture design without performing variations to the aggregate blend or just replaced the mineral filler (Bueno et al., 2019). As indicated by the G_{mm} values of the reference and μPCM-43 mixtures, a significant G_{mm} reduction is observed when μPCM is substituted for fine aggregates. Simultaneously, a lower amount of material is required to fabricate a desirable SGC specimen for the μPCM-43 mixtures relative to the reference mixture. Although replacing fine aggregate and mineral filler with μPCM-43 seems straightforward, such a change will cause a difference in volumetric properties and consequently mechanical performance.

5.2.2 Mechanical and Thermal Performance of μPCM-43 Mixture

To better understand the mechanical behavior of the μPCM-43 mixtures, the dynamic modulus for the redesigned asphalt mixtures was determined using two specimen geometries, namely 100-mm diameter by 150-mm tall (large specimen) and 38-mm diameter by 110-mm tall (small specimen). The ratio of stress to strain under vibratory conditions of large specimens was defined according to AASHTO T 378-17, while small specimen dynamic modulus testing was conducted according to AASHTO TP 132-19 (see Figure 5.1b). Additionally, the damage characteristic curve and fatigue analysis parameters of small specimens were estimated via the direct tension cyclic fatigue test, as specified by AASHTO TP 133-19. The big specimens were also measured for flow number to examine the resistance of the reference and μPCM-43 mixtures to permanent deformation. Finally, the fracture resistance of asphalt mixtures at low temperatures was characterized by means of the AASHTO T 394 test method. The specimens with a 150-mm diameter and 25-mm thickness were used to fabricate specimens for Semi-Circular Bend (SCB) geometry testing. Table 5.2 summarizes the asphalt mixture mechanical testing for this study. A PG 64-22 binder was used for all tests.

Figure 5.1 (a) 4% μPCM-43 mixture, 180-mm high SGC specimen and (b) dynamic modulus testing setup of small μPCM-43 mixture specimen.

TABLE 5.2
Asphalt mixture mechanical testing

Test Method	Reference Mixture	2% μPCM-43 Mixture	4% μPCM-43 Mixture
Dynamic Modulus Small Specimens, AASHTO TP 132	PG 64-22	PG 64-22	PG 64-22
Dynamic Modulus Big Specimens, AASHTO T 378	PG 64-22	PG 64-22	PG 64-22
Flow Number, AASHTO T 378	PG 64-22	PG 64-22	PG 64-22
Cyclic Fatigue Test, AASHTO TP 133	PG 64-22	PG 64-22	PG 64-22
Semi Circular Bend, AASHTO T 394	PG 64-22	PG 64-22	PG 64-22

Figure 5.2 (a) Insulation and instrumentation of specimens and (b) specimens of reference mixture and 4% μPCM-43 mixture in the environmental chamber.

In addition, the thermal response of μPCM-43 mixture specimens was investigated. The specimens were 100 mm (4 in.) in diameter and 50 mm (2 in.) thick and were instrumented with thermocouples and insulated, as shown in Figure 5.2. This part of the study analyzed the changes in temperature of a reference mixture specimen with 5% air voids content, 2% μPCM-43 mixture specimen having a 5% air voids content, and 4% μPCM-43 mixture specimens with 4%, 5%, and 6% air voids content under controlled environmental conditions (same thermal cycle as in Chapter 4, Section 4.3.2).

5.2.3 Rheological Performance of μPCM-43 Modified Binders

The mechanical characterization of μPCM-43 mixtures is complemented with rheological performance tests of μPCM-43 modified binders. As shown in Table 5.3, the properties of interest are the elastic response in an asphalt binder under shear creep and recovery, resistance to fatigue damage through cyclic loading, low-temperature relaxation, and the G* Change Rate (determined at 12°C/hr). The testing matrix included three types of original binder, PG 64-22, PG 70-22, and PG 76-22. The PG 64-22 is the same used for asphalt mixture testing. Initially, the μPCM-43 dosages of interest were 40% and 80% by binder mass because these percentages reflect the ratios of μPCM-43 to virgin binder in the μPCM-43 mixtures. However, the 80% μPCM dosage was not workable with stiff binders, making it impossible to prepare reliable binder specimens. Consequently, the dosages selected for μPCM-43 binder modification were 20% and 40% by binder mass, but data at an 80% μPCM-43 dosage was still gathered using PG 64-22 for DSR tests. All the tests were completed on original binder conditions, no Rolling Thin-Film Oven (RTFO) or Pressure Aging Vessel (PAV) aging protocols were performed.

5.3 Deliverables

5.3.1 Dynamic Modulus μPCM-43 Mixtures

As shown in Figure 5.3, a comparison of the dynamic modulus master curves of small specimens reveals that the reference mixture has a higher stiffness than the μPCM-43 mixtures, especially at the intermediate test temperatures (i.e., loading frequencies between 0.1 and 100 Hz). Previous studies have not discussed the reduction in dynamic modulus due to the presence of μPCM-43 particles (Bueno et al., 2019; Kakar et al., 2019a; 2019b; Refaa et al., 2018; Tian et al., 2019; Wei et al., 2019). Several investigations have implied that the decrease in temperature due to the thermal lag effect of μPCMs translates directly to a

TABLE 5.3
Testing matrix for asphalt binders with and without μPCM-43

Test Method	μPCM Dosage (by binder mass)		
	0%	20%	40%
Multiple Stress Creep Recovery (MSCR), AASHTO T 350	PG 64-22 PG 70-22 PG 76-22	PG 64-22 PG 70-22 PG 76-22	PG 64-22 PG 70-22 PG 76-22
Linear Amplitude Sweep (LAS), AASHTO T 101	PG 64-22 PG 70-22 PG 76-22	PG 64-22 PG 70-22 PG 76-22	PG 64-22 PG 70-22 PG 76-22
Delta Tc Parameter (ΔTc), ASTM D7643	PG 64-22 PG 70-22 PG 76-22	PG 64-22 PG 70-22 PG 76-22	PG 64-22 PG 70-22 PG 76-22
G* Change Rate	PG 64-22 PG 70-22 PG 76-22	PG 64-22 PG 70-22 PG 76-22	PG 64-22 PG 70-22 PG 76-22

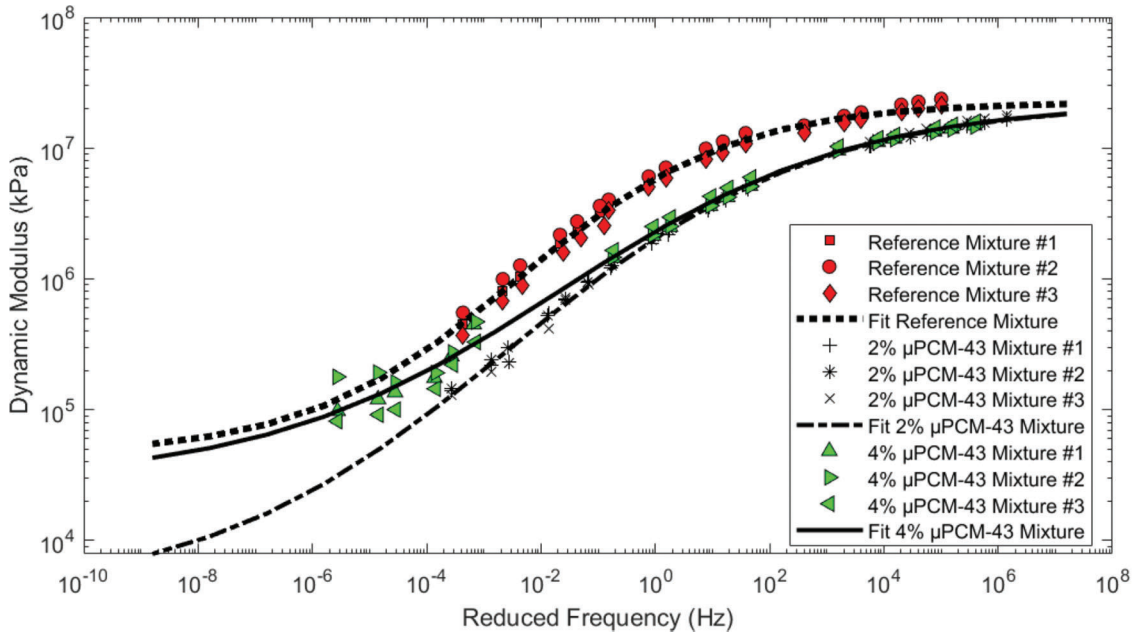

Figure 5.3 Dynamic modulus of reference and μPCM-43 mixtures, small specimens.

higher asphalt mixture or binder stiffness without acknowledging the mechanical impact of the μPCM-43 particles substitution of traditional mineral fillers. For conventional asphalt mixtures, some rules of thumb have been validated and can be used for quantifying the improvement of performance in asphalt mixtures due to temperature reduction (Si et al., 2015), where a slight shift in asphalt pavement temperature could lead to a significant increase in stiffness, or relaxation, and enhance pavement life-cycle performance. For example, a 5°C reduction in temperature can delay the risk of cracking for about 3 years (Si et al., 2015). However, the results presented herein suggest that these relationships should be validated for μPCM modified asphalt mixtures, as their mechanical behavior slightly shifts from conventional mixtures. The reduction in dynamic modulus may be associated with the stiffness, surface area properties, and interfacial adhesion of the μPCM particles. These factors should be further investigated through experimental testing and thermomechanical modeling, along with the thermal relaxation benefits that μPCM might provide.

The data suggest issues related to the repeatability and reproducibility of the test methods for the μPCM-43 mixtures at high temperatures. These results are consistent with laboratory observations. The dynamic modulus testing was conducted at three temperatures, 4°C, 20°C, and 40°C. During temperature conditioning and testing, a waxy appearance was noticed in the μPCM-43 mixture specimens at 40°C. Presumably, some of the capsules did not survive the mixing and specimen fabrication process, leading to paraffin leakage. As demonstrated by the DSC measurements, at temperatures below 38°C the core material of the

μPCM-43, paraffin, is a solid. But, at temperatures above of 38°C, it transforms into a liquid. The master curves were produced using the FlexMAT software, and comparable observations can be derived for big specimens. Overall, despite all the current limitations of the technology, the stiffness of μPCM-43 mixtures is not too dissimilar to a conventional asphalt mixture's behavior, as illustrated by the master curve analysis.

5.3.2 Permanent Deformation of μPCM-43 Modified Asphalt Materials

The test methods applied to evaluate the permanent deformation resistance of μPCM-43 modified asphalt binders and mixtures were the Multiple Stress Creep Recovery (MSCR) and Flow Number procedures. First, the MSCR results are presented in Table 5.4. The MSCR test has shown to be satisfactory for discriminating in identifying the rutting potential of both modified and neat binders. Lower nonrecoverable creep compliance of asphalt binder correlates to a better rutting performance. However, these data must be interpreted with caution because the measurements were performed on original binders. The MSCR method is intended for use with residue from the RTFO procedure. The results obtained suggest that the μPCM-43 particles act as a filler that stiffens the binder. The reduction in the nonrecoverable creep compliance parameters is consistent across the three binder types examined, and it depends on the amount of μPCM included in the asphalt binder specimens. The percentage differences with base binder and relative variability of the results are coherent, indicating a good affinity between the μPCM-43 particles and asphalt binders. The average nonrecoverable creep compliance reported for each experimental combination corresponds to the results obtained from three replicates. The stiffening effect of the μPCM-43 on the asphalt binders was also observed through high-temperature parameter ($G^*/\sin\delta$) binder grading.

Flow Number test results contrast with the MSCR results. Figure 5.4 shows that the Flow Number testing was conducted under unconfined testing conditions for the reference mixture and unconfined and confined environments for the 4% μPCM-43 mixture. Confining pressure was used for the μPCM-43 mixtures because

TABLE 5.4
Multiple stress creep recovery results for binders with and without μPCM-43

	Nonrecoverable Creep Compliance at 3.2 kPa, $Jnr_{3.2}$							
	μPCM Dosage (by binder mass)							
	0%		20%			40%		
Base Binder	Average (kPa^{-1})	CV (%)	Average (kPa^{-1})	CV (%)	Percentage Difference with Base Binder (%)	Average (kPa^{-1})	CV (%)	Percentage Difference with Base Binder (%)
PG 64-22	6.5	1.0	3.7	0.4	43.0	2.0	0.8	69.7
PG 70-22	5.6	0.5	2.5	0.6	56.0	1.8	0.6	68.1
PG 76-22	11.7	0.0	6.1	1.4	47.7	3.1	1.2	73.5

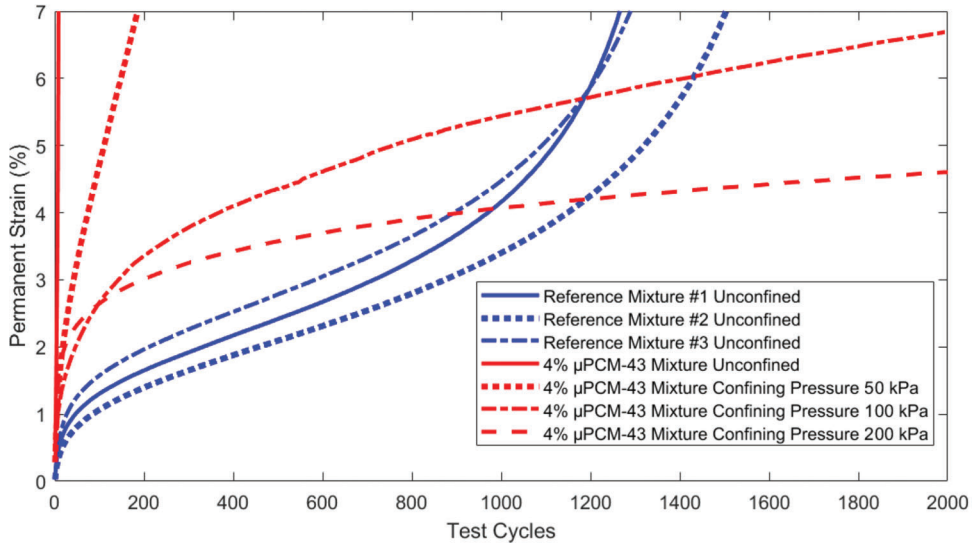

Figure 5.4 Flow number test results.

under unconfined testing conditions, the specimens will have failed immediately after a few cycles (permanent strain higher than 10%), as demonstrated by the 4% μPCM-43 mixture specimen tested unconfined. This outcome corroborated the suspicions that some PCM liquid might be leaking at high temperatures. The testing temperature for Flow Number evaluations was 53°C, a typical test parameter used for this method in Indiana. The permanent deformation results for the reference mixture specimens suggested an average Flow Number of 562 by fitting the experimental data to the Francken model. This average Flow Number satisfies the minimum criteria in AASHTO T 378 for a traffic level between 10 and 30 million ESALs. The Francken model approach also indicated that the Flow Number for the 4% μPCM-43 mixture specimens under a confining pressure of 50, 100, and 200 kPa was 2,076, 4,517, and 7,281, respectively. What emerges from the results reported in this section is that the μPCM-43 mixtures are susceptible to permanent deformation. Presumably, the loss of resistance to deformation under load is because of PCM leaking due to shell breakage during mixing and compaction, leading to a detrimental interaction between the PCM, asphalt binder, and aggregate materials, especially at temperatures above 40°C.

5.3.3 Fatigue Characteristics of μPCM-43 Modified Asphalt Mixtures.

The fatigue characteristics of base and μPCM-43 modified binders were characterized using the Linear Amplitude Sweep (LAS) test method described in AASHTO TP 101-14. The LAS tests were performed at temperature levels that could correlate with asphalt mixture testing (or the average of high and low PG temperatures minus 3°C), precisely 18°C for PG 64-22, 21°C for PG 70-22, and 24°C for PG 76-22. Table 5.5 reports the allowable binder fatigue life for 2.5% and 5.0% strain amplitudes, as determined by the asphalt binder fatigue model. The 5% strain amplitude used to predict the binder fatigue performance corresponds to a mixture strain of approximately 1,000με, which is typically considered a high strain level in pavements (Johnson, 2010). A lower strain amplitude of 2.5% is also reported in this portion of the study, as this strain level is typically used in similar investigations (Roque et al., 2020). The fatigue life analysis suggests that a lower resistance to cyclic loading should be expected for μPCM-43 modified asphalt binders in comparison to non μPCM modified binders. This decrement in fatigue resistance seems proportional to the amount of μPCM-43 modification and type of base binder.

Relatively speaking, the PG 76-22 binders with and without μPCM-43 outperformed the PG 64-22 and PG 70-22 binders at all μPCM dosages. Additionally, the percentages differences because of μPCM-43 modification are lower for PG 76-22 binders than PG 64-22 and PG 70-22 binders. This outcome implies that a shortage in fatigue performance due to μPCM-43 incorporation could be balanced using a base binder that better withstands damage accumulation caused by repetitive traffic loading. It should be noticed that the PG 76-22 showed the highest susceptibility to permanent deformation at all μPCM dosages when compared to the PG 64-22 and PG 70-22 binders.

Figure 5.5 illustrates the newly developed Cyclic Fatigue Index Parameter (S_{app}) for the materials under investigation for this research, reference and μPCM-43 mixtures, and for a mineral filler mixture. The mineral

TABLE 5.5
Fatigue life of binders with and without μPCM-43

	Fatigue Performance Parameter at 2.5% Applied Strain, N_f							
	μPCM Dosage (by binder mass)							
	0%		**20%**			**40%**		
Base Binder	**Average N_f**	**CV (%)**	**Average N_f**	**CV (%)**	**Percentage Difference with Base Binder (%)**	**Average N_f**	**CV (%)**	**Percentage Difference with Base Binder (%)**
PG 64-22	5,636	5.9	5,069	3.2	10.1	3,103	16.8	44.9
PG 70-22	4,386	5.2	3,587	17.3	18.2	1,730	5.4	60.6
PG 76-22	18,762	4.0	16,682	2.3	11.1	14,198	5.8	24.3
	Fatigue Performance Parameter at 5.0% Applied Strain, N_f							
	μPCM Dosage (by binder mass)							
	0%		**20%**			**40%**		
Base Binder	**Average N_f**	**CV (%)**	**Average N_f**	**CV (%)**	**Percentage Difference with Base Binder (%)**	**Average N_f**	**CV (%)**	**Percentage Difference with Base Binder (%)**
PG 64-22	807	4.9	661	5.1	18.1	425	15.0	47.4
PG 70-22	655	4.5	483	14.6	26.2	234	7.4	64.3
PG 76-22	2,867	1.5	2,622	2.4	8.6	2,328	6.9	18.8

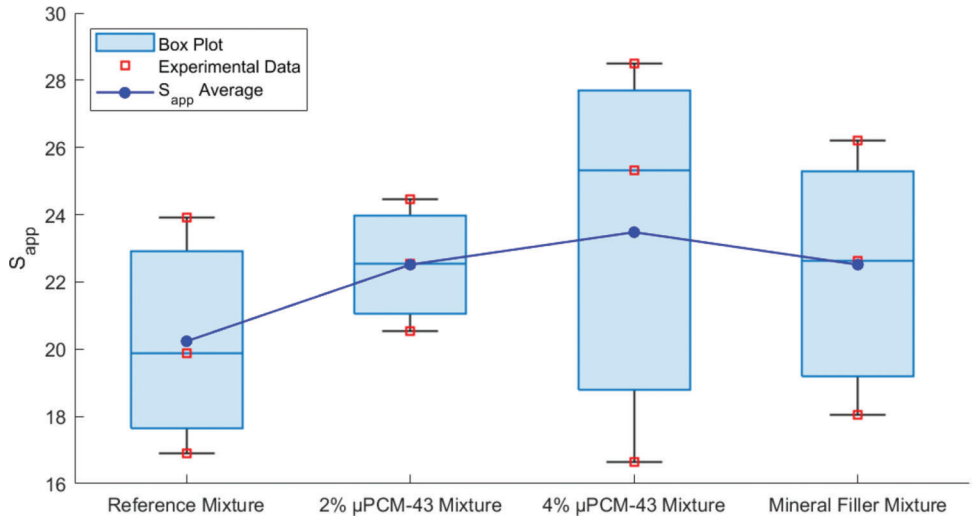

Figure 5.5 Cycling fatigue test results.

filler mixture contained a significant volume of fine particles, equivalent to the volume of μPCM particles in the 4% μPCM-43 mixture. In the mineral filler mixture, all the material passing the 0.600-mm sieve in the reference mixture was substituted with baghouse fines. This type of mixture was prepared to understand further the fatigue resistance of asphalt mixtures having a significant portion of fine particles. Three replicates are reported for each type of mixture. All the fatigue performance testing for this study was conducted at 18°C, as recommended by AASHTO TP 133. The average S_{app} results for the reference mixture, 2% μPCM-43 mixture, 4% μPCM-43 mixture and mineral filler mixture are 20.2, 22.5, 23.5, and 22.3, respectively. Considering that the S_{app} can distinguish the fatigue resistance of asphalt mixtures with varied properties (including aggregate gradation), the results demonstrate that the modifications performed to produce the μPCM-43 mixtures are not a concern for their fatigue performance. The μPCM-43 modified mixtures and mineral filler mixture provided slightly higher average S_{app} results compared to the reference mixture. The S_{app} accounts for the effects of a material's modulus and toughness on its fatigue resistance and is a measure of the amount of fatigue damage the material can tolerate under loading. Higher S_{app} values indicate better fatigue resistance of the mixture (Wang et al., 2020). Additionally, the S_{app} results of the μPCM-43 modified mixtures are similar to the values obtained for the mineral filler mixture, suggesting that at an intermediate temperature the microcapsules act as a conventional filler. The μPCM-43 particles inherently impact the fatigue resistance of the modified asphalt mixtures due to their characteristics, but no adverse effects are observed.

5.3.4 Low-Temperature Performance of μPCM-43 Modified Asphalt Materials

Table 5.6 reports the low-temperature characteristics of asphalt binders with and without μPCM-43 estimated using the Bending Beam Rheometer (BBR) test method (AASHTO T 313) at a testing temperature equal to -16°C and loading time of 60 s. The most striking observation that emerges from the data comparison is the dramatic increased in stiffness when the base binders are modified with μPCM-43. When the base asphalts are modified by 40% of total binder mass with μPCM-43, the stiffness can be doubled, raising concerns about the brittleness of μPCM-43 modified binders at low temperatures. This could be mitigated by a proper selection of base binder and μPCM-43 dosage. For instance, the control PG 70-22 binder's estimated stiffness is higher than PG 64-22 and PG 76-22 with a 20% μPCM-43 dosage. The relaxation properties of the base binders seem not to be as substantially influenced by the μPCM particles as the stiffness parameter. This behavior is in good agreement with the mechanical response of binders modified with any other filler having a comparable particle size distribution. Previous work suggests that although the stiffness increases due to the addition of fine particles in a binder matrix, the filler effect does not seriously hamper the ability of the system to dissipate energy by relaxation (Little & Petersen, 2005). These findings are confirmed by the Delta T_c parameter (ΔT_c) results, which suggest that the unaged binders with and without μPCM-43 are stiffness-controlled. All the ΔT_c values are between 0.5 and 2.2. The entire set of binders, which are unaged, appears far from the typically used ΔT_c warning level of -2.5°C (McDaniel & Shah, 2019). To calculate the ΔT_c parameter, three replicates were tested at -10°C, -16°C, -22°C, and -28°C using the BBR for each binder combination.

Figure 5.6 shows the stiffness results calculated from semi-circular asphalt mixture testing, according to AASHTO T 394. The stiffness is relatable to the elastic modulus of asphalt mixtures at low temperatures and calculated as the slope of the linear part of the ascending load-average line displacement ($P - u$) curve. The unit measure for this stiffness parameter is kN/mm.

TABLE 5.6
Low-temperature performance of binders with and without µPCM-43

	Estimated Stiffness at -16°C and 60 s, S							
	µPCM Dosage (by binder mass)							
	0%		20%			40%		
Base Binder	Average S (MPa)	CV (%)	Average S (MPa)	CV (%)	Percentage Difference with Base Binder (%)	Average S (MPa)	CV (%)	Percentage Difference with Base Binder (%)
PG 64-22	175.9	1.9	251.8	0.6	43.1	350.1	6.6	99.0
PG 70-22	275.5	7.6	385.1	3.6	39.8	493.1	7.2	79.0
PG 76-22	188.4	3.1	263.8	5.4	40.0	413.0	5.0	119.2
	m-value at -16°C and 60 s							
	µPCM Dosage (by binder mass)							
	0%		20%			40%		
Base Binder	Average m-value	CV (%)	Average m-value	CV (%)	Percentage Difference with Base Binder (%)	Average m-value	CV (%)	Percentage Difference with Base Binder (%)
PG 64-22	0.372	1.0	0.347	1.2	6.6	0.302	3.5	18.6
PG 70-22	0.323	3.4	0.302	0.3	6.5	0.273	2.9	15.6
PG 76-22	0.366	1.1	0.323	0.3	11.7	0.287	0.2	21.4
	Delta Tc Parameter, ΔT_c							
	µPCM Dosage (by binder mass)							
	0%		20%			40%		
Base Binder	Average ΔT_c	CV (%)	Average ΔT_c	CV (%)	Percentage Difference with Base Binder (%)	Average ΔT_c	CV (%)	Percentage Difference with Base Binder (%)
PG 64-22	1.5	15.9	1.6	12.4	8.1	1.3	22.4	12.2
PG 70-22	1.3	5.7	1.7	7.5	29.6	2.2	5.5	74.5
PG 76-22	1.2	10.6	0.5	70.1	56.5	1.3	13.2	13.2

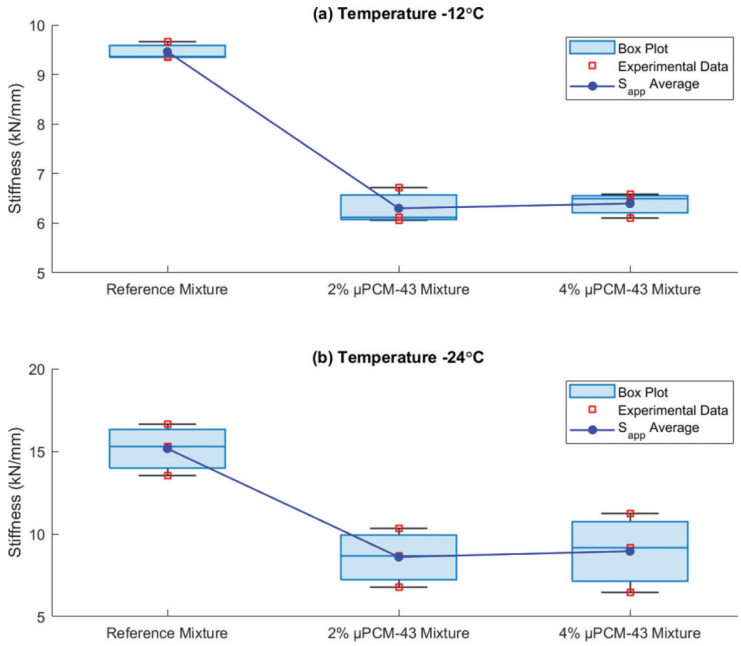

Figure 5.6 Stiffness results calculated from semicircular asphalt mixture testing.

The asphalt mixture low temperature response was determined at two levels, -12°C and -24°C. An increased asphalt mixture stiffness was observed at a lower testing temperature. The average stiffness parameters determined at -12°C of the reference, 2% μPCM-43, and 4% μPCM-43 mixtures are 9.5, 6.3, and 6.4 kN/mm, respectively. Whereas the average stiffness parameters achieved at -24°C of the reference, 2% μPCM-43 and 4% μPCM-43 mixtures are 15.2, 8.6, and 9.0 kN/mm, correspondingly. In addition, much more variability was observed in the stiffness results obtained at -24°C than at -12°C. However, the μPCM-43 effect found at both temperatures is the same. A sharp reduction in stiffness is observed when the μPCM-43 particles are incorporated into the asphalt mixtures at both fine aggregate replacement quantities, 2% and 4% by total mixture mass. The causes and implications of this finding need further research. But two interesting aspects can be derived from the achieved data. First, the fracture resistance of asphalt mixtures at low temperatures is altered with the inclusion of μPCM-43. Second, the stiffness parameter might be limited to discriminate among different levels of μPCM-43 modification, or a similar response is obtained regardless the amount of μPCM-43.

5.3.5 Thermal Response of μPCM-43 Modified Asphalt Materials

Figure 5.7 shows the thermal responses of the reference mixture, without μPCM, and the 4% μPCM-43 mixture with different air voids contents. The results resemble the thermal behavior of the μPCM-43 modified asphalt mixtures previously discussed, Mixtures A through D (see Figure 4.3), but the 4% μPCM-43 mixture has air voids contents within the acceptable air voids content range. The mixture was purposely redesigned to incorporate the μPCM without including an excessive amount of fine particles in the mixture (combination of fine aggregate, mineral filler, and μPCM).

Table 5.7 summarizes the results for both μPCM-43 mixtures and highlights the air voids content's importance to the temperature profile and heat flow within the μPCM-43 mixture specimens. More μPCM-43 particles in the mixture yield a higher temperature shift

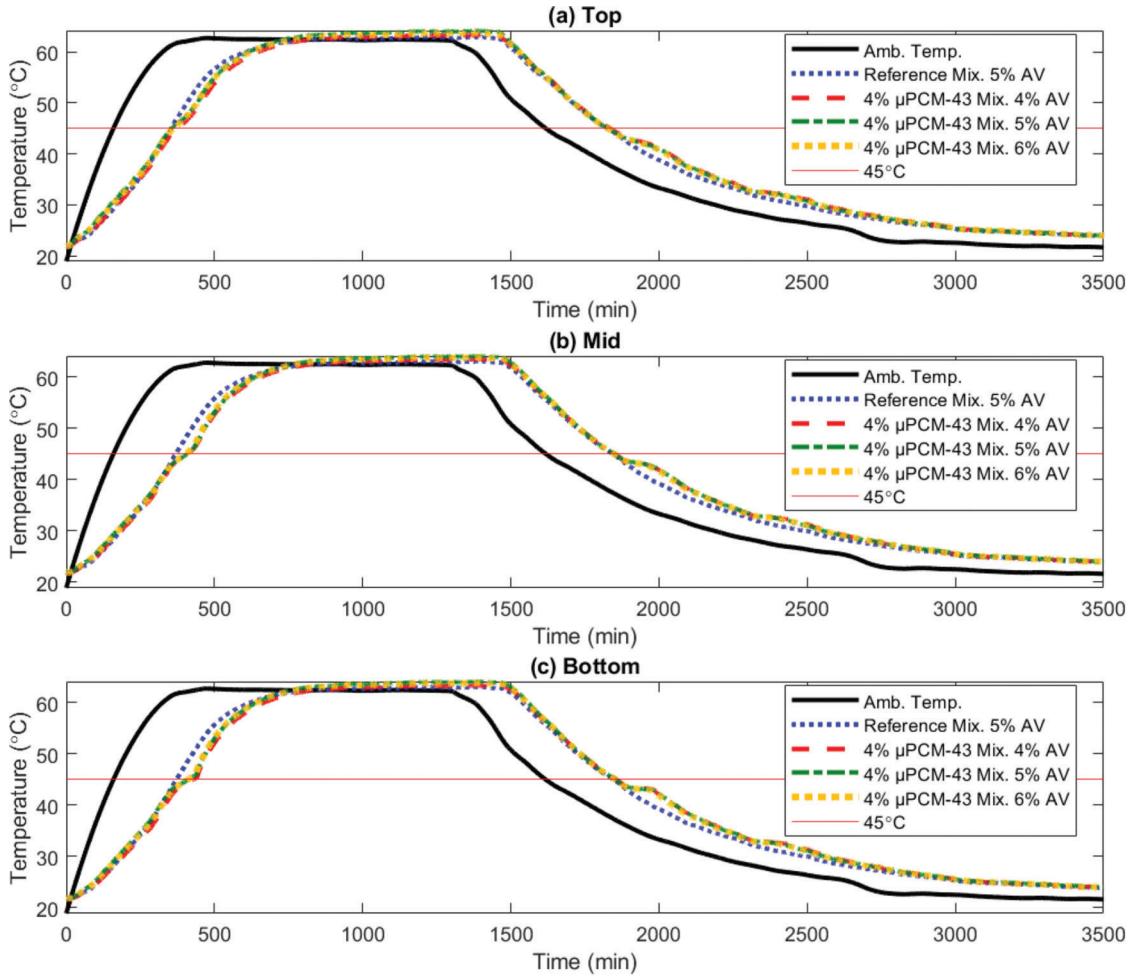

Figure 5.7 Thermal response of 4% μPCM-43 mixture specimens with various air voids contents at different depths from top surface.

TABLE 5.7
Absolute maximum temperature difference between reference mixture and μPCM-43 modified mixture specimens

Mixture Type	Air Voids Content (%)	Phase Transition	Absolute Maximum Temperature Difference (°C)		
			Depth from Top Surface (mm)		
			0 (Top Surface)	25 (Mid-Specimen)	50 (Bottom Surface)
4% μPCM-43 Mixture	4.0	Liquification	4.16	4.66	5.89
		Solidification	2.49	2.73	3.28
	5.0	Liquification	3.12	4.43	5.22
		Solidification	2.28	2.81	3.29
	6.0	Liquification	3.06	4.02	4.92
		Solidification	2.09	2.51	2.90
2% μPCM-43 Mixture	5.0	Liquification	2.49	3.06	3.92
		Solidification	1.48	1.72	2.01

between the mixture with and without μPCM. Furthermore, as the air voids content increases, the μPCM-43 effect seems to decrease, as demonstrated by the absolute maximum temperature difference between reference mixture and μPCM-43 mixture specimens. The average absolute temperature difference observed at the surface for all the μPCM-43 mixture specimens under liquification and solidification transitions is 2.65°C. This outcome agrees with the work reported in (Refaa et al., 2018), which through numerical analysis determined that replacing a similar portion of fine aggregate and mineral filler with μPCM could result in a reduction of the surface temperature of about 2.70°C.

It should be emphasized that all temperature differences are relative to the control reference mixture specimen which has an air voids content of 5%. However, the tendency is undeniable and corroborates previous research studying the effect of air voids content on thermal properties of asphalt mixtures. Hassn et al. (2016) determined that asphalt mixtures with high air voids contents have lower thermal conductivities and specific heat capacities than asphalt mixtures with lower air voids contents. Consequently, asphalt mixtures with high air voids contents are more suitable to alleviate the UHI effect. In contrast, asphalt mixtures with low air voids are recommended for harvesting solar energy from the environment. Given the results obtained for the 4% μPCM-43 mixture, it is plausible that slightly lower air voids contents might be more beneficial to maximize the μPCM effect.

5.3.6 Link Between Binder and Mixture Performance

As explained earlier, an attempt was made to identify the association between the binder and mixture results for μPCM modified asphalt materials. By modifying a PG 64-22 asphalt binder with μPCM-43 at 40% and 80% by binder mass (percentages that reflect the ratios of μPCM-43 to virgin binder in the μPCM-43 mixtures), the possible correlation between asphalt binder and mixture results was investigated. As has already been noted, the mechanical asphalt binder and mixture experiments provided compelling information about the behavior of μPCM modified asphalt materials. However, the experimental data gathered was insufficient to establish a correlation between the mechanical behavior of μPCM modified asphalt binder and mixtures; the μPCM particles influenced their mechanical responses in an ambivalent manner. Nevertheless, an interesting connection was found between the rheological response of μPCM-43 modified asphalt binders and the thermal response of μPCM-43 modified asphalt mixtures.

Figure 5.8 illustrates the link between the rheological testing for asphalt binders and thermal cycling results obtained for compacted asphalt mixtures. The absolute temperature difference plots delineate the gaps in temperature between the reference mixture and μPCM-43 mixture specimens with 5% air voids content. The disparities in temperature caused by the presence of μPCM have been the subject of investigation of previous studies (Ma et al., 2019; Si et al., 2015). Based on the fundamental theory of latent heat, Ma et al. (2019) proposed quantifying the accumulation of temperature difference between a μPCM asphalt mixture and non-μPCM modified asphalt mixture in a time range as a measurement of the μPCM modification effectiveness. The parameter's theoretical background suggests estimating the accumulated temperature difference (or area below the curve) as soon as a discrepancy is observed. Thus, Ma et al. (2019) failed to account for inherent temperature differences because of dissimilar material properties and proportions or thermocouple measurement errors. As can be seen in Figure 5.8, the differences in temperature below 1°C could be ignored as these disparities are not necessarily because of the latent heat effect of the μPCM.

To further assess the capability of the G* Change Rate, the rheological results reported in this section correspond to PG 64-22 asphalt binder specimens modified with μPCM at 0, 40, and 80% by total binder mass. These asphalt binder to μPCM ratios are in good agreement with the raw quantities of material included in the μPCM-43 mixtures (see Table 5.1). The G* Change Rate was determined by conducting DSR tests at 12°/hr. The number, shape, and intensity of the G*

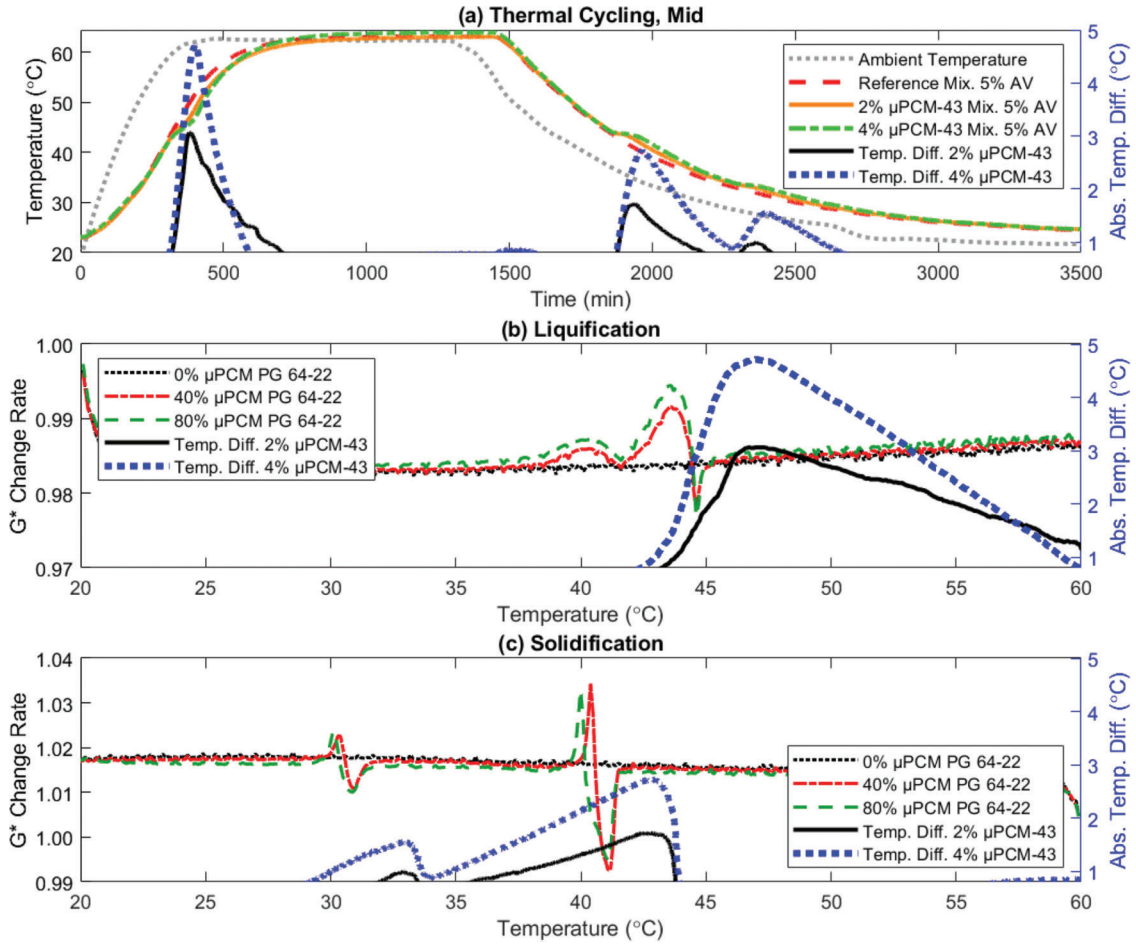

Figure 5.8 Relationship between rheological measurements and thermal cycling experiments.

Change Rate peaks are analogous to the temperature difference curves observed between the reference mixture and μPCM-43 mixture specimens. As previously reported, the thermal peak in the PCM liquification transition is more uniform, generating a higher temperature difference than the solidification transition. When the paraffin material inside the μPCM-43 is crystallizing, the latent heat effect is divided in two parts as confirmed in Figure 5.8c. It should be highlighted that as more μPCM-43 particles are included in the DSR testing, the G* Change Rate slighlty drifts from the baseline, or G* Change Rate reported by the control PG 64-22 binder specimen. However, the concept is still applicable. Similar observations can be made for PG 70-22 and PG 76-22 asphalt binders modified with μPCM-43.

6. CONCLUSIONS AND RECOMMENDATIONS

6.1 Summary and Conclusions

This study attempts to understand the environmental tuning of asphalt pavement materials using PCM. The relevance of PCM modified asphalt binders and mixtures is supported by the current findings available in the literature. The work presented herein advances the environmental tuning of asphalt pavement materials using μPCM and is significant, because it establishes a rheological measurement and mixture design method for μPCM incorporation in asphalt binders and mixtures. By strategically modifying asphalt binders and mixtures, optimum dosages of μPCM in asphalt paving materials is feasible. Additionally, this research provides a substantial amount of information about the synthetization, characterization, and encapsulation of PCM for paving purposes. The thermal and mechanical tuning of asphalt materials to their anticipated environment is expected to improve asphalt mixture performance and extend asphalt pavement service life, leading to more sustainable paving technologies. The following conclusions can be drawn from the present study.

- The synthesis of FAAms from different commercial vegetable oils and primary alkyl-amines was carried out, and their chemical and thermal properties were studied. Based on green chemistry metrics focused on maximizing resources, the synthesized materials have the potential to be used as PCMs. More work is needed to determine the feasibility FAAms PCMs for asphalt applications.

- This study introduces a ball milling experimental procedure to examine the survivability of μPCM particles during the production of asphalt mixtures. The results suggest that close to 90% of the capsules can survive abrasive forces at room temperature. Additionally, thermal stability tests complemented with image analysis indicate that μPCM is stable at asphalt production temperatures (between 135°C–162°C, or 275°F–325°F). However, the combined effects of mixing temperatures and abrasive forces are still a concern and subject of future investigations.
- Rheological measurements using the DSR equipment can help identify the latent heat effect of μPCM particles in asphalt binders. This study's findings propose the use of the G* Change Rate parameter to determine the temperatures at which the μPCM effect occurs. This approach can also provide insights into the intensity of the μPCM impact on asphalt mixtures.
- The experimental results confirm that μPCM modified asphalt mixture specimens can experience temperature differences between 1.8°C and 10.3°C lower, as compared to non-μPCM modified asphalt mixture specimens subjected to the same ambient temperatures. In practice, this suggests that μPCM can delay the appearance of undesirable temperatures in asphalt pavements. However, this outcome depends on the amount and characteristics of μPCM, asphalt mixture materials, ambient temperature, phase change transition (solidification or liquification), depth from the pavement surface, and density of the compacted asphalt mixture.
- DSR and DSC results verify that asphalt binder viscoelastic flow is a thermally activated process. The rate at which asphalt binder stiffness changes is conditional on the temperature fluctuations experienced by the material.
- The asphalt binder and mixture mechanical test results suggest ambivalent performance outcomes caused by the incorporation of μPCM in asphalt paving materials. Taken together, the mechanical analysis indicates that the μPCM particles could behave like a conventional mineral filler if they suffer no damage during mixing and compaction.

6.2 Recommendations

This research study's overall significance should not be limited to the optimum characterization and design of μPCM asphalt materials. The widespread implementation of μPCM modified asphalt pavements can potentially benefit not only the pavement performance but society, as well. As demonstrated by this study, the environmental tuning of asphalt materials using μPCM could mitigate the appearance of the intense surface and inner temperatures on asphalt pavements, which could help alleviate the UHI effect. Consequently, this research's findings could positively impact various areas, such as transportation safety and electricity demand. Accordingly, this study provides the following insights for future research.

- Future work is needed to evaluate the survivability of μPCM during the production, placement, and compaction of asphalt materials. In addition, the long-term performance of the μPCM capsules under repetitive vehicle loading and temperature fluctuations must be assessed.
- Although this study has progressed the design of μPCM mixtures, several assumptions still required validation. In particular, the mixture design approach suggests replacing a portion of fine aggregate and mineral filler with μPCM capsules by volume. Nevertheless, the specific gravity and absorption properties of the replaced materials and μPCM particles should be further characterized to define an appropriate compaction level and establish a reliable mixture design procedure.
- A countereffect in the viscoelastic flow of μPCM modified asphalt binders was found based on the G* Change Rate analysis. Therefore, a natural progression of this work is to determine the causes and possible implications of this finding.
- Future implementation of asphalt pavements modified with PCMs will required design and quality assurance procedures beyond volumetric, rheological and mechanical methods. Further research should explore the degree to which chemical, thermal, and visual techniques could be used to provide confidence that quality requirements are fulfilled.
- Although many aspects related to the tuning of asphalt pavements with PCMs are still in flux, the implementation of pavements with intrinsic thermal resistance properties is expected to evolve quickly. Therefore, despite its limitations, this research work adds understanding to this growing area of study and recommends close monitoring of emerging technologies that could help with the temperature management of pavements.
- Further research should encourage the construction of field trials that demonstrate the modification of asphalt materials with μPCM. Such a process could help validate and address μPCM modified asphalt pavements' benefits, design, and challenges. The additional costs related to the use of μPCM particles will be hard to justify without reliable field performance histories.

REFERENCES

Agyenim, F., Hewitt, N., Eames, P., & Smyth, M. (2010). A review of materials, heat transfer and phase change problem formulation for latent heat thermal energy storage systems (LHTESS). *Renewable and Sustainable Energy Reviews*, *14*(2), 615–628. https://doi.org/10.1016/j.rser.2009.10.015

Anderson, D. A., Christensen, D. W., Bahia, H. U., Dongre, R., Sharma, M. G., Antle, C. E., & Button, J. (1994). *Binder characterization and evaluation, volume 3: Physical characterization* (Strategic Highway Research Report No. SHRP-A-369). Strategic Highway Research Program.

Asphalt Institute Foundation. (2017, December). *STAR symposium report 2017.* Retrieved March 16, 2020, from https://bookstore.asphaltinstitute.org/STAR17report

Aydin, A. A., & Aydin, A. (2012). High-chain fatty acid esters of 1-hexadecanol for low temperature thermal energy storage with phase change materials. *Solar Energy Materials and Solar Cells*, *96*(1), 93–100. https://doi.org/10.1016/J.SOLMAT.2011.09.013

Baetens, R., Jelle, B. P., & Gustavsen, A. (2010). Phase change materials for building applications: A state-of-the-art review. *Energy and Buildings*, *42*(9), 1361–1368. https://doi.org/10.1016/j.enbuild.2010.03.026

Behnood, A., Shah, A., McDaniel, R. S., & Olek, J. (2016). *Analysis of the multiple stress creep recovery asphalt binder test and specifications for use in Indiana* (Joint Transportation Research Program Publication No. FHWA/IN/JTRP-2016/07). West Lafayette, IN: Purdue University. https://doi.org/10.5703/1288284316330

Behzadi, S., & Farid, M. M. (2014). Long term thermal stability of organic PCMs. *Applied Energy*, *122*, 11–16. https://doi.org/10.1016/j.apenergy.2014.01.032

Betancourt-Jimenez, D., Youngblood, J. P., & Martinez, C. J. (2020). Synthesis and characterization of fatty acid amides from commercial vegetable oils and primary alkyl amines for phase change material applications. *ACS Sustainable Chemistry and Engineering*, *8*(36), 13683–13691. https://doi.org/10.1021/acssuschemeng.0c03626

Bilyk, A., Bistline Jr., R. G., Piazza, G. J., Feairheller, S. H., & Haas, M. J. (1992, May). A novel technique for the preparation of secondary fatty amides. *Journal of the American Oil Chemists' Society*, *69*(5), 488–491. https://doi.org/10.1007/BF02540956

Bueno, M., Kakar, M. R., Refaa, Z., Worlitschek, J., Stamatiou, A., & Partl, M. N. (2019). Modification of asphalt mixtures for cold regions using microencapsulated phase change materials. *Scientific Reports*, *9*(1), 1–10. https://doi.org/10.1038/s41598-019-56808-x

Bureau of Naval Personnel. (1966). *Principles of naval engineering*. Superintendent of Documents, U.S. Government Printing Office.

Burrows, A., Holman, J., Parsons, A., Pilling, G., & Price, G. (2013). *Chemistry^3: introducing inorganic, organic and physical chemistry*. Oxford University Press.

Cabeza, L. F., Zsembinszki, G., & Martín, M. (2020). Evaluation of volume change in phase change materials during their phase transition. *Journal of Energy Storage*, *28*, 101206. https://doi.org/10.1016/j.est.2020.101206

Cao, X., Tang, B., Zhu, H., Zhang, A., & Chen, S. (2011). Cooling principle analyses and performance evaluation of heat-reflective coating for asphalt pavement. *Journal of Materials in Civil Engineering*, *23*(7), 1067–1075. https://doi.org/10.1061/(ASCE)MT.1943-5533.0000256

Cebula, D. J., & Smith, K. W. (1991, August). Differential scanning calorimetry of confectionery fats. Pure triglycerides: Effects of cooling and heating rate variation. *Journal of the American Oil Chemists Society*, *68*(8), 591–595. https://doi.org/10.1007/BF02660159

Chen, M. Z., Hong, J., Wu, S. P., Lu, W., & Xu, G. J. (2011). Optimization of phase change materials used in asphalt pavement to prevent rutting. In H. Zhang, G. Shen, D. Jin (Eds.), *Advanced Materials Research*, *219–220*, 1375–1378. https://doi.org/10.4028/www.scientific.net/AMR.219-220.1375

Chen, M., Wan, L., & Lin, J. (2012). Effect of phase-change materials on thermal and mechanical properties of asphalt mixtures. *Journal of Testing and Evaluation*, *40*(5), 2012 0091. https://doi.org/10.1520/JTE20120091

Constable, D. J. C., Curzons, A. D., & Cunningham, V. L. (2002). Metrics to 'green' chemistry—which are the best? *Green Chemistry: An International Journal and Green Chemistry Resource: GC*, *4*(6), 521–527. https://doi.org/10.1039/B206169B

Dickinson, E., & McClements, D. (1996). *Advances in food colloids*. Blackie Academic & Professional.

Dicks, A. P., & Hent, A. (2015). *Green chemistry metrics*. Springer International Publishing. https://doi.org/10.1007/978-3-319-10500-0

Dutil, Y., Rousse, D. R., Ben Salah, N., Lassue, S., & Zalewski, L. (2011). A review on phase-change materials: Mathematical modeling and simulations. *Renewable and Sustainable Energy Reviews*, *15*(1), 112–130. https://doi.org/10.1016/j.rser.2010.06.011

Farid, M. M., Khudhair, A. M., Razack, S. A. K., & Al-Hallaj, S. (2004). A review on phase change energy storage: materials and applications. *Energy Conversion and Management*, *45*(9–10), 1597–1615. https://doi.org/10.1016/J.ENCONMAN.2003.09.015

Flagella, Z., Rotunno, T., Tarantino, E., Di Caterina, R., & De Caro, A. (2002). Changes in seed yield and oil fatty acid composition of high oleic sunflower (Helianthus annuus L.) hybrids in relation to the sowing date and the water regime. *European Journal of Agronomy*, *17*(3), 221–230. https://doi.org/10.1016/S1161-0301(02)00012-6

Fleischer, A. S. (2015). *Thermal energy storage using phase change materials: Fundamentals and applications*. Springer International Publishing.

Floros, M. C., & Narine, S. S. (2016). Latent heat storage using renewable saturated diesters as phase change materials. *Energy*, *115*(Part 1), 924–930. https://doi.org/10.1016/J.ENERGY.2016.09.085

Guan, B., Ma, B., & Fang, Q. (2011). Application of asphalt pavement with phase change materials to mitigate urban heat island effect. *2011 International Symposium on Water Resource and Environmental Protection*, 2389–2392. IEEE. https://doi.org/10.1109/ISWREP.2011.5893749

Gui, J. G., Phelan, P. E., Kaloush, K. E., & Golden, J. S. (2007). Impact of pavement thermophysical properties on surface temperatures. *Journal of Materials in Civil Engineering*, *19*(8), 683–690. https://doi.org/10.1061/(ASCE)0899-1561(2007)19:8(683)

Haddock, J. E., Rahbar-Rastegar, R., Pouranian, M. R., Montoya, M., & Patel, H. (2020). *Implementing the Superpave 5 asphalt mixture design method in Indiana* (Joint Transportation Research Program Publication No. FHWA/IN/JTRP-2020/12). West Lafayette, IN: Purdue University. https://doi.org/10.5703/1288284317127

Hassn, A., Aboufoul, M., Wu, Y., Dawson, A., & Garcia, A. (2016). Effect of air voids content on thermal properties of asphalt mixtures. *Construction and Building Materials*, *115*, 327–335. https://doi.org/10.1016/j.conbuildmat.2016.03.106

He, L. H., Li, J. R., & Zhu, H. Z. (2013). Analysis on application prospect of shape-stabilized phase change materials in asphalt pavement. *Applied Mechanics and Materials*, *357–360*, 1277–1281. https://doi.org/10.4028/www.scientific.net/AMM.357-360.1277

Incropera, F. P., DeWitt, F. P., Bergman, T. L., & Lavine, A. S. (Eds.) (2007). *Fundamentals of heat and mass transfer* (6th ed.). John Wiley.

Jamekhorshid, A., Sadrameli, S. M., & Farid, M. (2014). A review of microencapsulation methods of phase change materials (PCMs) as a thermal energy storage (TES) medium. *Renewable and Sustainable Energy Reviews*, *31*, 531–542. https://doi.org/10.1016/j.rser.2013.12.033

Jin, J., Lin, F., Liu, R., Xiao, T., Zheng, J., Qian, G., Liu, H., & Wen, P. (2017). Preparation and thermal properties of mineral-supported polyethylene glycol as form-stable composite phase change materials (CPCMs) used in asphalt pavements. *Scientific Reports*, *7*(1), 1–10. https://doi.org/10.1038/s41598-017-17224-1

Johnson, C. M. (2010). *Estimating asphalt binder fatigue resistance using an accelerated test method* [Doctoral dissertation, University of Wisconsin-Madison]. http://digital.library.wisc.edu/1793/46799

Kakar, M. R., Refaa, Z., Bueno, M., Worlitschek, J., Stamatiou, A., & Partl, M. N. (2020). Investigating bitumen's direct interaction with Tetradecane as potential phase change material for low temperature applications. *Road Materials and Pavement Design*, *21*(8), 2356–2363. https://doi.org/10.1080/14680629.2019.1601127

Kakar, M. R., Refaa, Z., Worlitschek, J., Stamatiou, A., Partl, M. N., & Bueno, M. (2019a, September). Effects of aging on asphalt binders modified with microencapsulated phase change material. *Composites Part B: Engineering*, *173*, 107007. https://doi.org/10.1016/j.compositesb.2019.107007

Kakar, M. R., Refaa, Z., Worlitschek, J., Stamatiou, A., Partl, M. N., & Bueno, M. (2019b, August). Thermal and rheological characterization of bitumen modified with microencapsulated phase change materials. *Construction and Building Materials*, *215*, 171–179. https://doi.org/10.1016/j.conbuildmat.2019.04.171

Kalnæs, S. E., & Jelle, B. P. (2015, May). Phase change materials and products for building applications: A state-of-the-art review and future research opportunities. *Energy and Buildings*, *94*, 150–176. https://doi.org/10.1016/j.enbuild.2015.02.023

Kenisarin, M., & Mahkamov, K. (2007, December). Solar energy storage using phase change materials. *Renewable and Sustainable Energy Reviews*, *11*(9), 1913–1965. https://doi.org/10.1016/J.RSER.2006.05.005

Keshavarz, M. H., Akbarzadeh, A. R., Rahimi, R., Jafari, M., Pasandideh, M., & Sadeghi, R. (2016, November). A reliable method for prediction of enthalpy of fusion in energetic materials using their molecular structures. *Fluid Phase Equilibria*, *427*, 46–55. https://doi.org/10.1016/J.FLUID.2016.06.052

Kheradmand, M., Castro-Gomes, J., Azenha, M., Silva, P. D., De Aguiar, J. L. B., & Zoorob, S. E. (2015, August). Assessing the feasibility of impregnating phase change materials in lightweight aggregate for development of thermal energy storage systems. *Construction and Building Materials*, *89*, 48–59. https://doi.org/10.1016/j.conbuildmat.2015.04.031

Knothe, G., & Kenar, J. A. (2004). Determination of the fatty acid profile by ^{1}H-NMR spectroscopy. *European Journal of Lipid Science and Technology*, *106*(2), 88–96. https://doi.org/10.1002/ejlt.200300880

Kodippily, S., Yeaman, J., Henning, T., & Tighe, S. (2018). Effects of extreme climatic conditions on pavement response. *Road Materials and Pavement Design*, *21*(5), 1413–1425. https://doi.org/10.1080/14680629.2018.1552620

Kousksou, T., Jamil, A., El Rhafiki, T., & Zeraouli, Y. (2010). Paraffin wax mixtures as phase change materials. *Solar Energy Materials and Solar Cells*, *94*(12), 2158–2165. https://doi.org/10.1016/J.SOLMAT.2010.07.005

Lajara, J. R., Diaz, U., & Quidiello, R. D. (1990, October). Definite influence of location and climatic conditions on the fatty acid composition of sunflower seed oil. *Journal of the American Oil Chemists' Society*, *67*(10), 618–623. https://doi.org/10.1007/BF02540410

Lane, G. (2018). *Solar heat storage: Volume I: Latent heat materials*. CRC Press.

Lavigne, F., Bourgaux, C., & Ollivon, M. (1993, December). Phase transitions of saturated triglycerides. *Le Journal de Physique IV*, *03*(C8), C8-137–C8-140. https://doi.org/10.1051/jp4:1993825

Liston, L. C., Farnam, Y., Krafcik, M., Weiss, J., Erk, K., & Tao, B. Y. (2016). Binary mixtures of fatty acid methyl esters as phase change materials for low temperature applications. *Applied Thermal Engineering*, *96*, 501–507. https://doi.org/10.1016/j.applthermaleng.2015.11.007

Little, D. N., & Petersen, J. C. (2005). Unique effects of hydrated lime filler on the performance-related properties of asphalt cements: Physical and chemical interactions revisited. *Journal of Materials in Civil Engineering*, *17*(2), 207–218. https://doi.org/10.1061/(asce)0899-1561(2005)17:2(207)

Ma, B., Chen, S.-S., Wei, K., Liu, F.-W., & Zhou, X.-Y. (2019). Analysis of thermoregulation indices on micro-encapsulated phase change materials for asphalt pavement. *Construction and Building Materials*, *208*, 402–412. https://doi.org/10.1016/j.conbuildmat.2019.03.014

Mallick, R. B., Radzicki, M. J., Daniel, J. S., & Jacobs, J. M. (2014). Use of system dynamics to understand long-term impact of climate change on pavement performance and maintenance cost. *Transportation Research Record*, *2455*(1), 1–9. https://doi.org/10.3141/2455-01

Mandelkern, L. (2002). *Crystallization of polymers*. Cambridge University Press.

Manning, B. J., Bender, P. R., Cote, S. A., Lewis, R. A., Sakulich, A. R., & Mallick, R. B. (2015). Assessing the feasibility of incorporating phase change material in hot mix asphalt. *Sustainable Cities and Society*, *19*, 11–16. https://doi.org/10.1016/j.scs.2015.06.005

McDaniel, R. S., & Shah, A. (2019). *Investigation of delta Tc for implementation in Indiana* (Joint Transportation Research Program Publication No. FHWA/IN/JTRP-2019/14). West Lafayette, IN: Purdue University. https://doi.org/10.5703/1288284316923

Microtek Laboratories. (n.d.). *Nextek 43 microcapsules technical sheet*. https://www.microteklabs.com/product-data-sheets/

Mondal, S. (2008). Phase change materials for smart textiles–An overview. *Applied Thermal Engineering*, *28*(11–12), 1536–1550. https://doi.org/10.1016/j.applthermaleng.2007.08.009

Montoya, M. A., Rahbar Rastegar, R., & Haddock, J. E. (2021) *Incorporating phase change materials in asphalt pavements to melt snow and ice* [Manuscript submitted for publication]. Lyles School of Civil Engineering, Purdue University.

Naresh, R., Parameshwaran, R., & Vinayaka Ram, V. (2020). Bio-based phase-change materials. *Bio-Based Materials and Biotechnologies for Eco-Efficient Construction*, 203–242. Woodhead Publishing Series in Civil and Structural Engineering. https://doi.org/10.1016/B978-0-12-819481-2.00011-8

O'Neil, G. W., Yen, T. Q., Leitch, M. A., Wilson, G. R., Brown, E. A., Rider, D. A., & Reddy, C. M. (2019). Alkenones as renewable phase change materials. *Renewable Energy*, *134*, 89–94. https://doi.org/10.1016/J.RENENE.2018.11.001

Oró, E., de Gracia, A., Castell, A., Farid, M. M., & Cabeza, L. F. (2012). Review on phase change materials (PCMs) for cold thermal energy storage applications. *Applied Energy*, *99*, 513–533. https://doi.org/10.1016/j.apenergy.2012.03.058

Papagiannakis, A. T., & Masad, E. A. (2008). *Pavement design and materials*. John Wiley & Sons.

Pardauil, J. J. R., de Molfetta, F. A., Braga, M., de Souza, L. K. C., Filho, G. N. R., Zamian, J. R., & da Costa, C. E. F. (2017). Characterization, thermal properties and phase transitions of amazonian vegetable oils. *Journal of Thermal Analysis and Calorimetry*, *127*(2), 1221–1229. https://doi.org/10.1007/s10973-016-5605-5

Raghunanan, L., Floros, M. C., & Narine, S. S. (2016). Thermal stability of renewable diesters as phase change materials. *Thermochimica Acta*, *644*, 61–68. https://doi.org/10.1016/J.TCA.2016.10.009

Ravotti, R., Fellmann, O., Lardon, N., Fischer, L. J., Stamatiou, A., & Worlitschek, J. (2018). Synthesis and investigation of thermal properties of highly pure carboxylic fatty esters to be used as PCM. *Applied Sciences*, *8*(7), 1069. https://doi.org/10.3390/app8071069

Ray, E., Kandhal, P. S., Roberts, F. L., Kim, Y. R., Lee, D.-Y., Kennedy, T. W. (2009). *Hot mix asphalt materials, mixture design, and construction* (3rd ed.). NAPA Educational Foundation.

Refaa, Z., Kakar, M. R., Stamatiou, A., Worlitschek, J., Partl, M. N., & Bueno, M. (2018). Numerical study on the effect of phase change materials on heat transfer in asphalt concrete. *International Journal of Thermal Sciences*, *133*(March), 140–150. https://doi.org/10.1016/j.ijthermalsci.2018.07.014

Rohman, A., & Che Man, Y. B. (2012). Quantification and classification of corn and sunflower oils as adulterants in olive oil using chemometrics and FTIR spectra. *The Scientific World Journal*, 2012, 1–6. https://doi.org/10.1100/2012/250795

Roque, R., Yan, Y., & Lopp, G. (2020, June). *Evaluation of the cracking performance of asphalt binders at intermediate temperatures*. Florida Department of Transportation.

Roschangar, F., Sheldon, R. A., & Senanayake, C. H. (2015). Overcoming barriers to green chemistry in the pharmaceutical industry–the Green Aspiration Level^{TM} concept. *Green Chemistry*, *17*(2), 752–768. https://doi.org/10.1039/C4GC01563K

Safar, M., Bertrand, D., Robert, P., Devaux, M. F., & Genot, C. (1994). Characterization of edible oils, butters and margarines by Fourier transform infrared spectroscopy with attenuated total reflectance. *Journal of the American Oil Chemists' Society*, *71*(4), 371–377. https://doi.org/10.1007/BF02540516

Sharma, A., Tyagi, V. V., Chen, C. R., & Buddhi, D. (2009). Review on thermal energy storage with phase change materials and applications. *Renewable and Sustainable Energy Reviews*, *13*(2), 318–345. https://doi.org/10.1016/j.rser.2007.10.005

Sheldon, R. A. (2018). Metrics of green chemistry and sustainability: Past, present, and future. *ACS Sustainable Chemistry & Engineering*, *6*(1), 32–48. https://doi.org/10.1021/acssuschemeng.7b03505

Si, W., Zhou, X.-Y., Ma, B., Li, N., Ren, J. P., & Chang, Y.-J. (2015). The mechanism of different thermoregulation types of composite shape-stabilized phase change materials used in asphalt pavement. *Construction and Building Materials*, *98*, 547–558. https://doi.org/10.1016/j.conbuildmat.2015.08.038

Sun, L. (2016). *Structural behavior of asphalt pavements*. Butterworth-Heinemann Elsevier.

Stauffer, E., Dolan, J., & Newman, R. (2008). *Fire debris analysis* (1st ed.). Academic Press.

Tan, C. P., & Che Man, Y. B. (2002, May/June). Comparative differential scanning calorimetric analysis of vegetable oils: I. Effects of heating rate variation. *Phytochemical Analysis*, *13*(3), 129–141. https://doi.org/10.1002/pca.633

Tian, Y.-X., Ma, B., Liu, F.-W., Li, N., & Zhou, X.-Y. (2019). Thermoregulation effect analysis of microencapsulated phase change thermoregulation agent for asphalt pavement. *Construction and Building Materials*, *221*, 139–150. https://doi.org/10.1016/j.conbuildmat.2019.05.184

Vo, H. V., Park, D.-W., & Dessouky, S. (2015). Simulation of snow melting pavement performance using measured thermal properties of graphite-modified asphalt mixture. *Road Materials and Pavement Design*, *16*(3), 696–706. https://doi.org/10.1080/14680629.2015.1020847

Wang, Y. D., Underwood, B. S., & Kim, Y. R. (2020). Development of a fatigue index parameter, S_{app}, for asphalt mixes using viscoelastic continuum damage theory. *The International Journal of Pavement Engineering*, *23*(2), 438–452. https://doi.org/10.1080/10298436.2020.1751844

Wei, K., Wang, Y., & Ma, B. (2019). Effects of microencapsulated phase change materials on the performance of asphalt binders. *Renewable Energy*, *132*, 931–940. https://doi.org/10.1016/j.renene.2018.08.062

Yang, H., Tian, R., & Li, Y. (2008). Organic reactions catalyzed by 1, 4-diazabicyclo [2.2.2] octane (DABCO). *Frontiers of Chemistry in China*, *3*(3), 279–287. https://doi.org/10.1007/s11458-008-0049-5

Yavuzturk, C., Ksaibati, K., & Chiasson, A. D. (2005). Assessment of temperature fluctuations in asphalt pavements due to thermal environmental conditions using a two-dimensional, transient finite-difference approach. *Journal of Materials in Civil Engineering*, *17*(4), 465–475. https://doi.org/10.1061/(asce)0899-1561(2005)17:4(465)

Yusoff, N. I. M., Shaw, M. T., & Airey, G. D. (2011). Modelling the linear viscoelastic rheological properties of bituminous binders. *Construction and Building Materials*, *25*(5), 2171–2189. https://doi.org/10.1016/j.conbuildmat.2010.11.086

Zalba, B., Marín, J. M., Cabeza, L. F., & Mehling, H. (2003). Review on thermal energy storage with phase change: materials, heat transfer analysis and applications. *Applied Thermal Engineering*, *23*(3), 251–283. https://doi.org/10.1016/S1359-4311(02)00192-8

Zambiazi, R. C., Przybylski, R., Zambiazi, M. W., & Mendonça, C. B. (2007). Fatty acid composition of vegetable oils and fats. *Boletim Do Centro de Pesquisa de Processamento de Alimentos*, *25*(1), 111–120

APPENDICES

Appendix A. Chemical and Thermal Characterization of FAAms Synthesized from Corn, Sunflower, and Palm Oils

Appendix B. Thermal Cycling Results Mixture B through D

APPENDIX A. CHEMICAL AND THERMAL CHARACTERIZATION OF FAAMS SYNTHESIZED FROM CORN, SUNFLOWER, AND PALM OILS

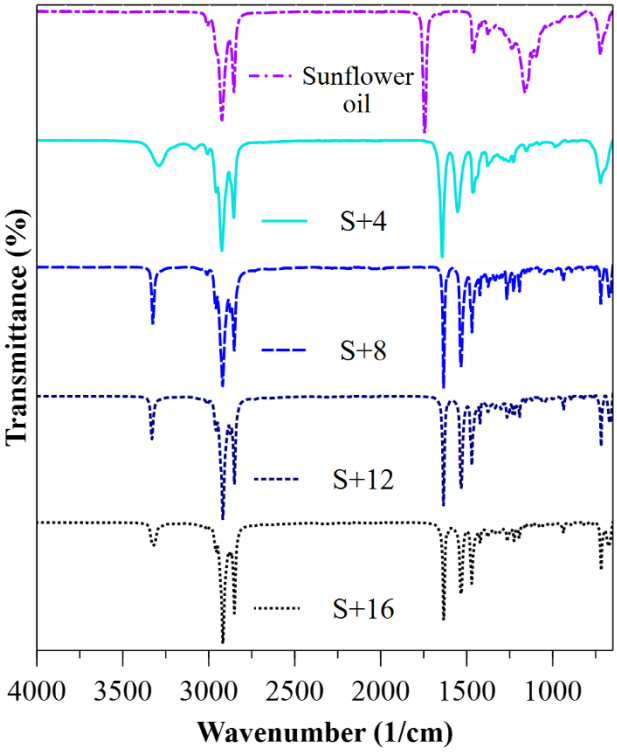

Figure A.1 FT-IR spectra of sunflower oil and fatty acid amides (FAAms) from sunflower oil and butylamine (S+4), sunflower oil and octylamine (S+8), sunflower oil and dodecylamine (S+12) and sunflower oil and hexadecylamine (S+16).

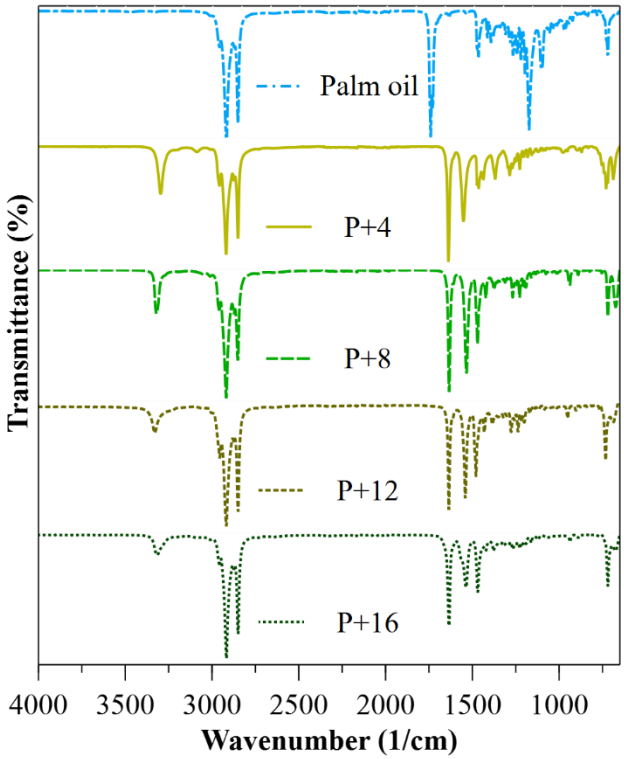

Figure A.2 FT-IR spectra of palm oil and fatty acid amides (FAAms) from palm oil and butylamine (P+4), palm oil and octylamine (P+8), palm oil and dodecylamine (P+12) and palm oil and hexadecylamine (P+16).

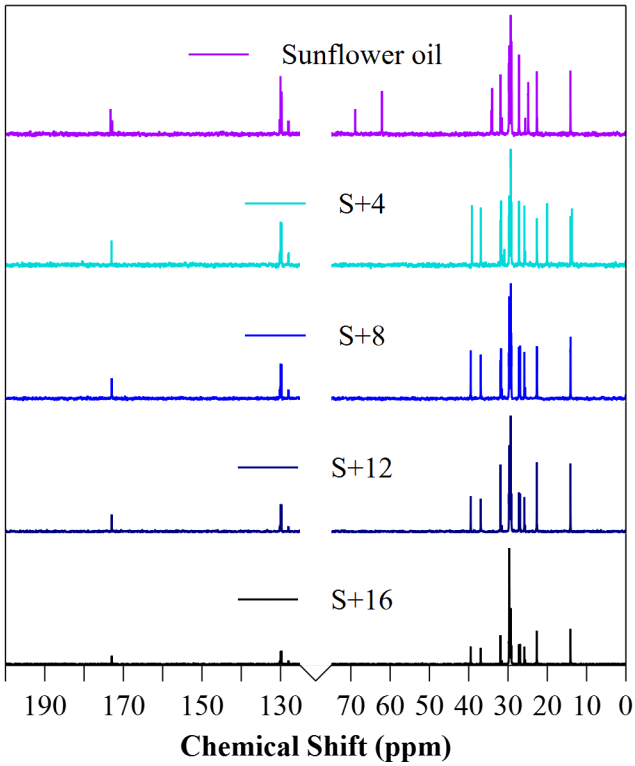

Figure A.3 ^{13}C NMR spectra of sunflower oil and fatty acid amides from sunflower oil and butylamine (S+4), sunflower oil and octylamine (S+8), sunflower oil and dodecylamine (S+12), and sunflower oil and hexadecylamine (S+16).

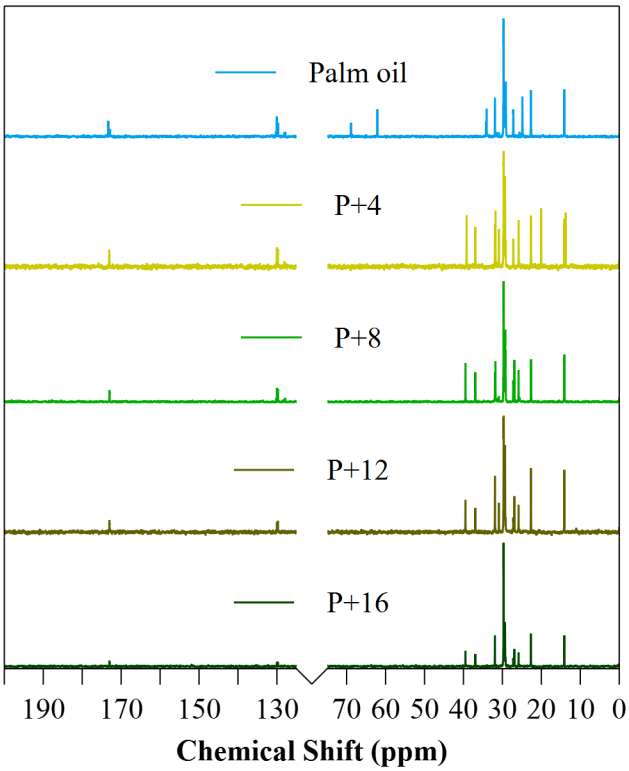

Figure A.4 ^{13}C NMR spectra of palm oil and fatty acid amides from palm oil and butylamine (P+4), palm oil and octylamine (P+8), palm oil and dodecylamine (P+12), and palm oil and hexadecylamine (P+16).

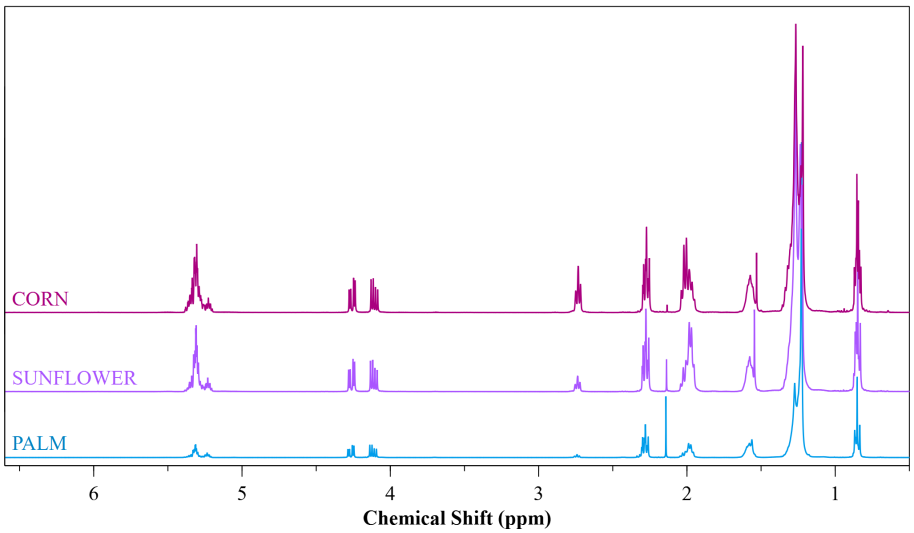

Figure A.5 ^{1}H NMR spectra of corn, sunflower, and palm oil samples.

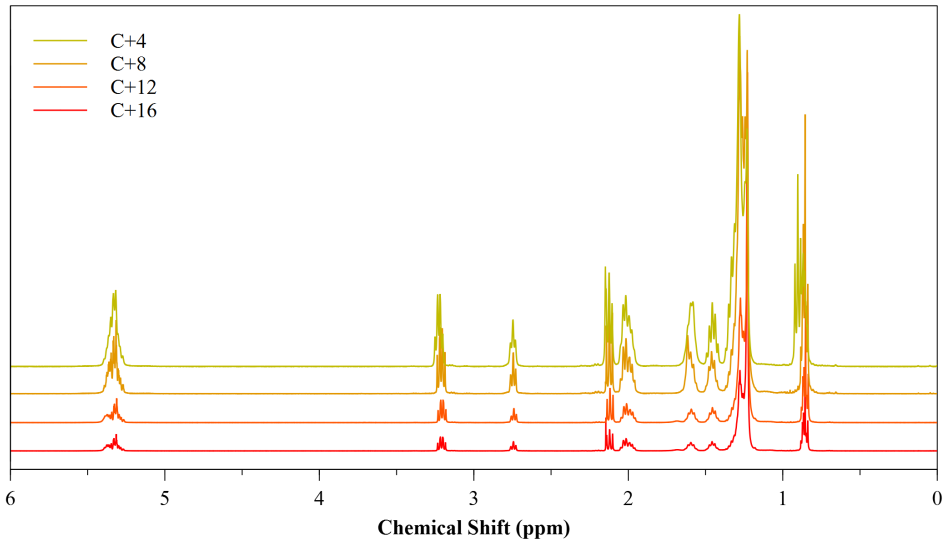

Figure A.6 ^{1}H NMR spectra of FAAms synthesized from corn oil and butylamine (C+4), corn oil and octylamine (C+8), corn oil and dodecylamine (C+12), and corn oil and hexadecylamine (C+16).

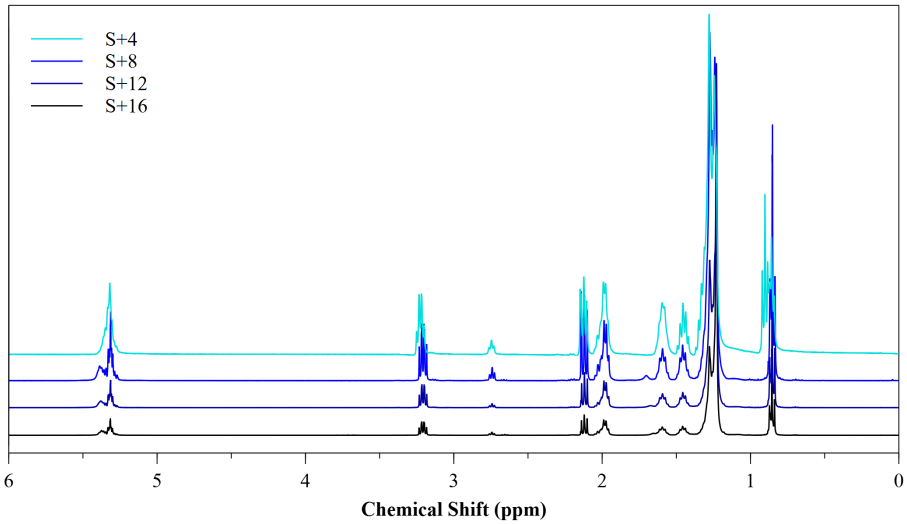

Figure A.7 ^{1}H NMR spectra of FAAms synthesized from sunflower oil and butylamine (S+4), sunflower oil and octylamine (S+8), sunflower oil and dodecylamine (S+12), and sunflower oil and hexadecylamine (S+16).

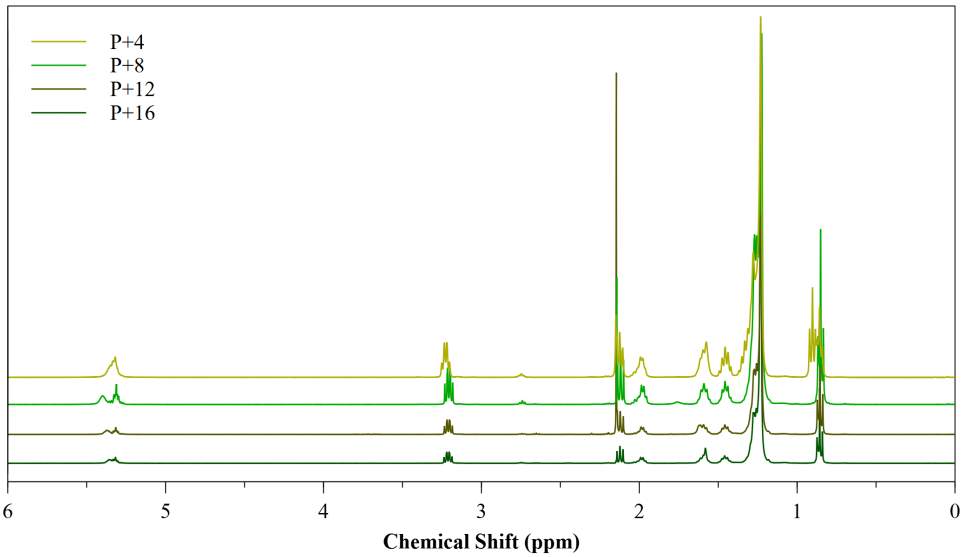

Figure A.8 ^{1}H NMR spectra of FAAms synthesized from palm oil and butylamine (S+4), sunflower oil and octylamine (S+8), sunflower oil and dodecylamine (S+12), and sunflower oil and hexadecylamine (S+16).

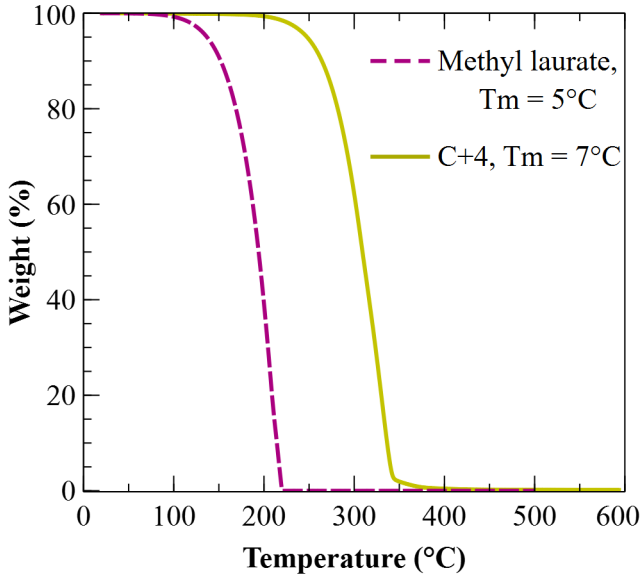

Figure A.9 TGA diagram of methyl laurate and FAAms from corn oil and butylamine (C+4).

APPENDIX B. THERMAL CYLING RESULTS MIXTURE B THROUGH D

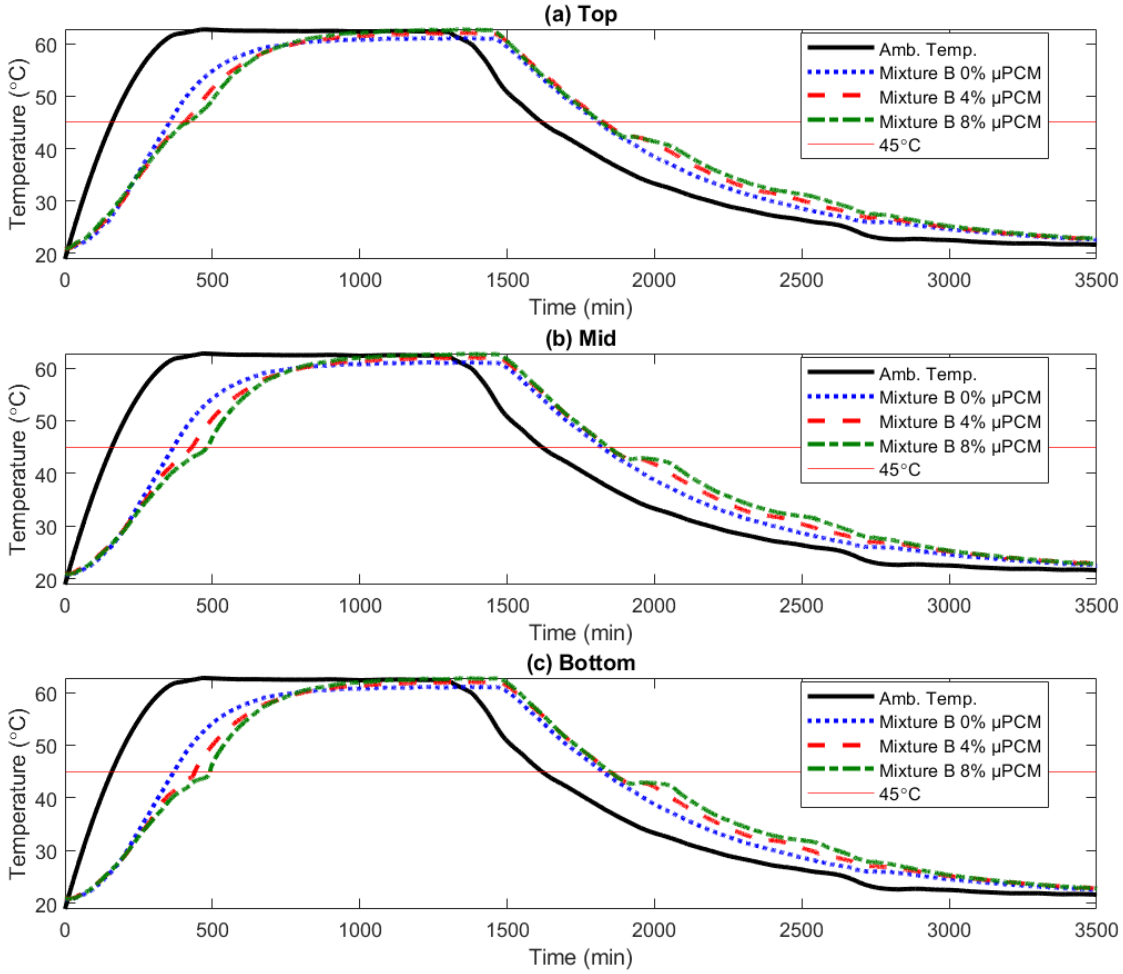

Figure B.1 Mixture B thermal response of asphalt specimens with and without µPCM-43 at different depths from top surface.

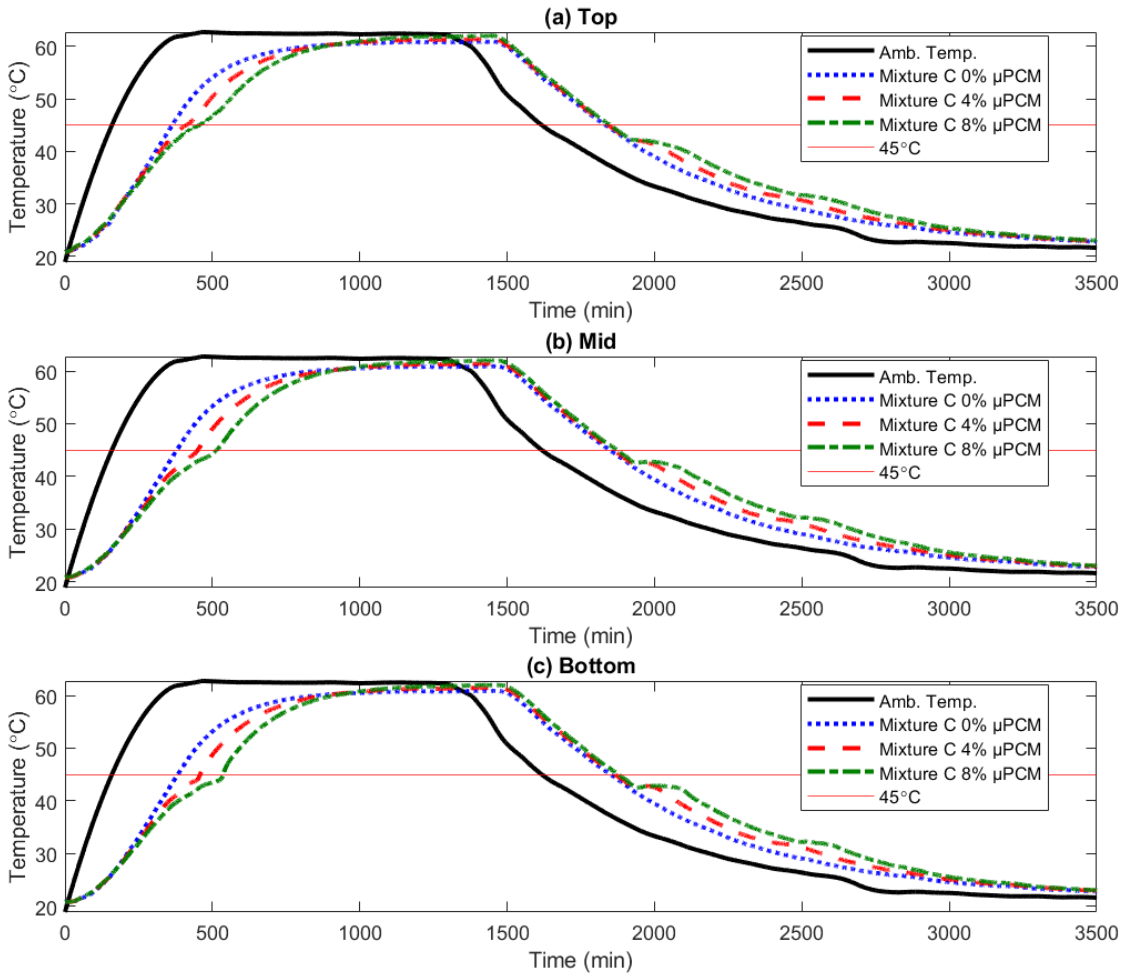

Figure B.2 Mixture C thermal response of asphalt specimens with and without µPCM-43 at different depths from top surface.

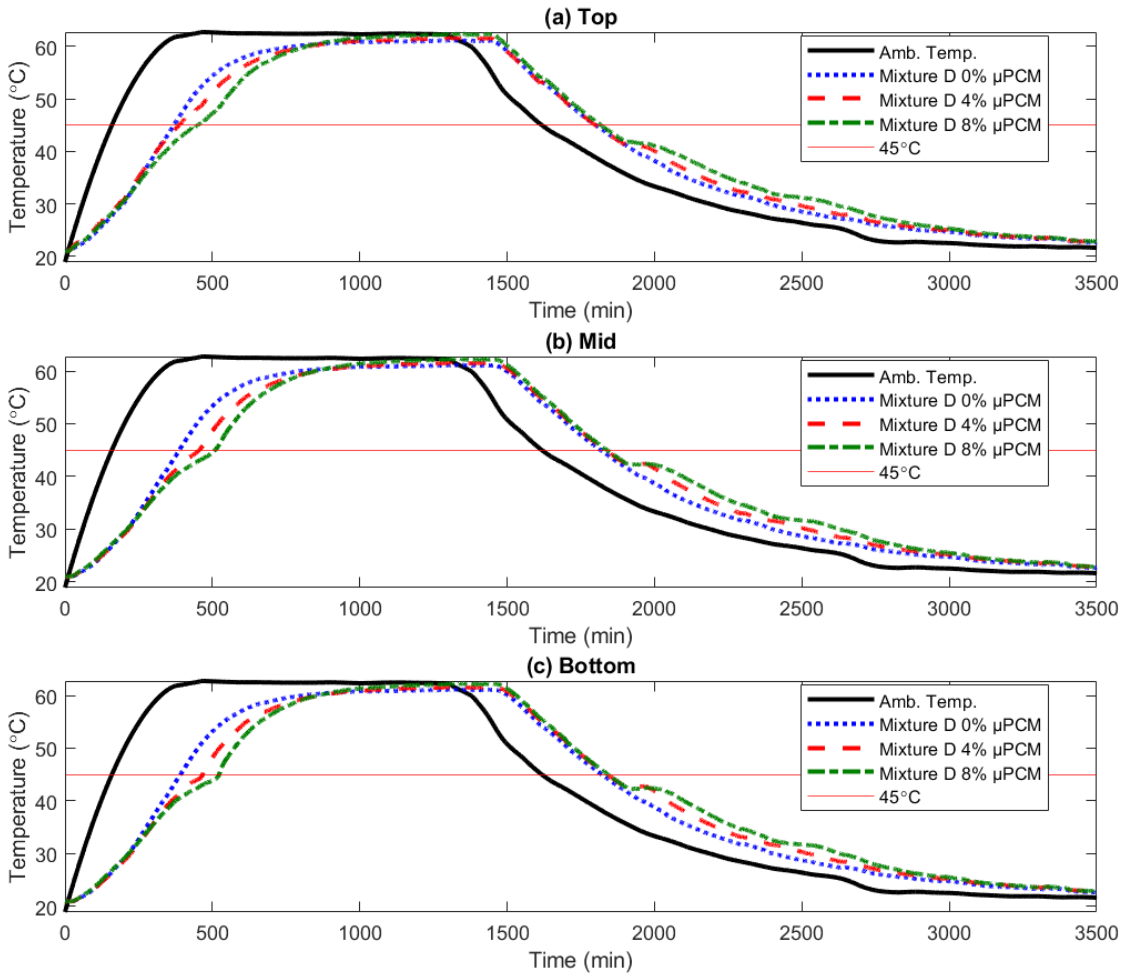

Figure B.3 Mixture D thermal response of asphalt specimens with and without µPCM-43 at different depths from top surface.

About the Joint Transportation Research Program (JTRP)

On March 11, 1937, the Indiana Legislature passed an act which authorized the Indiana State Highway Commission to cooperate with and assist Purdue University in developing the best methods of improving and maintaining the highways of the state and the respective counties thereof. That collaborative effort was called the Joint Highway Research Project (JHRP). In 1997 the collaborative venture was renamed as the Joint Transportation Research Program (JTRP) to reflect the state and national efforts to integrate the management and operation of various transportation modes.

The first studies of JHRP were concerned with Test Road No. 1—evaluation of the weathering characteristics of stabilized materials. After World War II, the JHRP program grew substantially and was regularly producing technical reports. Over 1,600 technical reports are now available, published as part of the JHRP and subsequently JTRP collaborative venture between Purdue University and what is now the Indiana Department of Transportation.

Free online access to all reports is provided through a unique collaboration between JTRP and Purdue Libraries. These are available at http://docs.lib.purdue.edu/jtrp.

Further information about JTRP and its current research program is available at http://www.purdue.edu/jtrp.

About This Report

An open access version of this publication is available online. See the URL in the citation below.

Montoya, M. A., Betancourt-Jimenez, D., Notani, M., Rahbar-Rastegar, R., Youngblood, J. P., Martinez, C. J., & Haddock, J. E. (2022). *Environmentally tuning asphalt pavements using phase change materials* (Joint Transportation Research Program Publication No. FHWA/IN/JTRP-2022/06). West Lafayette, IN: Purdue University. https://doi.org/10.5703/1288284317369